Applied Catalysis B: Environmental 170-171 (2015) 241–254

Contents lists available at ScienceDirect

Applied Catalysis B: Environmental

journal homepage: www.elsevier.com/locate/apcatb

Cu-substituted ZSM-5 catalyst: Controlling of $DeNO_x$ reactivity via ion-exchange mode with copper–ammonia solution

Svetlana Yashnik[a,*], Zinfer Ismagilov[a,b]

[a] Boreskov Institute of Catalysis, Novosibirsk, Russia
[b] Institute of Coal Chemistry and Materials Science, Kemerovo, Russia

ARTICLE INFO

Article history:
Received 11 September 2014
Received in revised form
27 December 2014
Accepted 17 January 2015
Available online 20 January 2015

Keywords:
Cu–ZSM-5
Copper-substituted zeolite
Copper–ammonia complex
Copper-oxide structure with extra-lattice oxygen
$DeNO_x$ reaction

ABSTRACT

The regularities of sorption and stabilization of Cu^{2+} ions in Cu–ZSM-5 catalysts prepared via the ion-exchange have been studied. The copper sorption by H–, Na–, and NH_4–ZSM-5 from aqueous and ammonia solutions of copper salt had a good approximation as the Langmuir mould of a monolayer adsorption. At ideal ion-exchange condition, only the isolated copper ions located in the zeolite ion-exchange position are formed. Observation of other Cu structures with extra-lattice oxygen is a result of the hydrolysis of hexaaquacopper(II) complex and its polycondensation reactions. They exist as (1) dimer and copper-oxide structures with chain-like and square-planar coordination of extra-lattice oxygen ligands, which are located inside zeolite channels, and (2) oxide clusters and CuO nanoparticles dispersed on the zeolite crystallite surface.

The RedOx properties and $DeNO_x$ reactivity in selective catalytic reduction of nitrogen oxide by propane of copper-substituted ZSM-5 have been compared. The dynamics of $DeNO_x$ reactivity correlates with the growth in the number of the isolated Cu^{2+} ions and the Cu structures with extra-lattice oxygen, which are formed during the ion exchange of H–ZSM-5 with water–ammonia solutions of copper acetate with NH_4OH/Cu^{2+} close to 6 (pH ~ 10.5). On the other hand, reactivity decreases with an increase in the content of copper-oxide clusters on the external surface of zeolite, which are observed in the ion-exchanged Cu–ZSM-5 at NH_4OH/Cu^{2+} below 6. Besides, the Cu^{2+} ions stabilized during the ion-exchange mode with strong-alkaline ammonia–copper solution ($NH_4OH/Cu^{2+} = 30$) are less reducible in H_2-TPR experiment compared with catalysts produced from ammonia-free and weak-ammonia solution of copper acetate, probably due to the low copper loading, stabilization of isolated Cu^{2+}_{Oh} ions with large distance between each other, decoration of copper ions by a thin silica/alumina layer or formation of Cu-silicates.

1. Introduction

Starting from the works by Iwamoto et al. [1] and Held et al. [2], who have discovered the unique catalytic activity of Cu–ZSM-5 zeolites in the direct decomposition of nitrogen oxides and their selective reduction by hydrocarbons, interest in the copper-containing catalysts still persists. Up to date, various research groups have been involved in investigation of the active state of copper ions [3,4], a search for new catalytic reactions with participation of Cu–ZSM-5 [5,6], and development of advanced methods for the synthesis of copper-containing catalysts [7–9]. Although post-synthetic modification of zeolites was considered in many works, ion exchange remains the most widely used method of Cu–ZSM-5 synthesis; this is caused by the simplicity of its technical implementation, reproducibility of the catalyst properties, and a higher catalytic activity of the ion-exchanged catalysts [9]. Numerous ion exchange techniques have been reported; however, the regularities of ion exchange in dependence on its main parameters are discussed quite rarely [4,10–13]. As for the works devoted to catalytic activity of Cu–ZSM-5, they consider mostly the correlations with catalytically active states of copper ions, which include the isolated copper ions [14–16], copper ion structures with extra-lattice oxygen [3,4,9,10,17] and even the oxide nanoparticles [18,19]. Nevertheless, data on the correlations between ion exchange conditions and predominant states of copper ions formed in this process are very essential because they can be used for deliberate control of the catalytic characteristics of Cu–ZSM-5 in a wide series of RedOx reactions.

The liquid-phase ion exchange is carried out by immersion of the H–, Na– or NH_4– form of ZSM-5 zeolite in aqueous solutions of

* Corresponding author. Tel.: +10 383 330 66 81; fax: +10 383 330 62 19.
E-mail address: yashnik@catalysis.ru (S. Yashnik).

http://dx.doi.org/10.1016/j.apcatb.2015.01.021
0926-3373/

copper acetate [4,10,20], nitrate [4,10,13], chloride [4,9,10] or sulfate [4,10,21]. The duration of the ion exchange commonly ranges from 12 to 48 hours. After the ion exchange, samples are filtered, washed with water, and heat treated. Copper content in the copper-substituted zeolites is characterized by the calculated value of atomic ratio Cu/Al_{at} or the exchange level. The exchange level (as a percentage) is calculated on the basis of a 1Cu–2Al stoichiometry [1]. In this case, $Cu/Al_{at} = 0.5$ corresponds formally to a 100% substitution of protons in Si(OH)Al groups of zeolite by the Cu^{2+} ions; however, this is not always possible even at the perfectly chosen ion exchange conditions.

Copper content in the Cu–ZSM-5 samples synthesized by the ion exchange from aqueous solutions of copper salts, except for copper acetate, is usually much lower than the Cu/Al = 0.50; the main copper state in such catalysts corresponds to isolated copper ions stabilized in the cation exchange positions of the zeolite. To increase copper content of Cu–ZSM-5, the ion exchange procedures are repeated 3–5 times [13], and ammonia is introduced in the aqueous slurry of zeolite powder and copper salts after the ion exchange procedure [12,17]. Sometimes, for increasing of copper loading of Cu–ZSM-5, the copper–ammonia solutions are used for the ion-exchange with H–ZSM-5 [4,13]. In the latter case, the copper exchange level can reach value as high as 200–400% [1,4,13]. For the over-exchanged Cu–ZSM-5, the predominant copper state corresponds to copper dimers ($[Cu–O–Cu]^{2+}$, [10,17]), bis(μ-oxo) dicopper $[Cu–(O)_2–Cu]^{2+}$ [3] and chain-like copper-oxide structures [4] inside the zeolite channels and highly dispersed copper-oxide clusters on the zeolite surface [9,18,19].

When both the aqueous and ammonia solutions of copper salts are used, the most pronounced effect on the copper content and its electronic state is exerted by the following ion exchange parameters: copper concentration in the solution [4,13], pH of the solution [4,10–13], atomic ratio of silicon to aluminum in the zeolite matrix [4,13], and temperature of the ion exchange [22]. However, ion exchange isotherms and chemistry of the processes that take place at the ion exchange between copper salt solutions and H–ZSM-5 zeolite are discussed very rarely in the literature; systematic data on the effect of ion exchange parameters on the properties of Cu–ZSM-5 are virtually absent.

In the present work, we have studied the main regularities of copper cation sorption by H–ZSM-5 zeolite from aqueous and water-ammonia solutions of copper acetate as function of ammonia to copper concentration ratio. The electronic state of copper ions and their RedOx properties on Cu–ZSM-5 were studied by UV–vis DR spectroscopy, ESR, and hydrogen temperature-programmed reduction (H_2-TPR), respectively. The obtained data were compared to their catalytic reactivity in the NO selective catalytic reduction by propane (NO SCR-C_3H_8) to reveal the main correlations.

2. Experimental

2.1. Catalyst preparation

Cu–ZSM-5 samples were prepared by the ion exchange of parent H–ZSM-5 (*Si/Al* = 17) with aqueous and ammonia solutions of copper acetate, which had pH close to 5.7 and 10.5–11.5, respectively. Copper concentrations were varied in the range of 0.5–8 g Cu/l. The ammonia solutions of copper acetate were prepared by addition of ammonia solution to aqueous copper acetate solution in the amount corresponding to the NH_4OH/Cu^{2+} molar ratio equal to 3, 6, 15, and 30. In some experiments, NH_4CH_3COO (77 g/l or 1 M) was added to copper acetate solutions in order to maintain the ionic force of the solution.

Sorption of copper cations was investigated by the fractional sampling method. Zeolite mass was 1 g. The slurry concentration (the ratio of the solution volume to the zeolite mass, S/Z) was 10. After 48 h of the ion exchange at room temperature, the zeolite samples were filtered and washed with distilled water or ammonia solution with pH 10.5. The sample washing was stopped when a blue coloring of wash water at ammonia addition has vanished. All the samples were dried at 110 °C and calcined in air at 500 °C.

After the ion exchange, the equilibrium concentrations of copper in the solution and in the zeolite were analyzed. The copper content in the ion-exchange solution was determined by spectrophotometric method using a Shimadzu UV-2501 PC spectrophotometer. The copper loading in the as-prepared Cu–ZSM-5 samples was determined by the atomic emission spectrometry using the inductively coupled plasma method (ICP-AES Instrument, Perkin–Elmer Optima DV-3300). The data obtained were approximated by the Langmuir equation for monomolecular adsorption model:

$$A = A_{\max} \frac{k_s \times C}{1 + k_s \times C}, \quad (1)$$

where A is the copper amount adsorbed on ZSM-5 (solid) from solution at a given copper concentration; A_{max} is the maximum copper amount adsorbed by ZSM-5 when all sorption positions are occupied; k_s is the Langmuir equilibrium constant, and C is the equilibrium concentration of copper ions in solution.

Below, the samples are denoted as *n*% Cu(α)ZSM-5-X, where *n*% is the copper content (wt.%), α is the formal molar ratio of NH_4OH to Cu^{2+}, ZSM-5 is the zeolite structure, and *X* is the copper-exchange level. The sample prepared from the solutions with ammonium acetate addition contains in its designation *, for example 1.7% Cu(6*)ZSM-5–0.33.

2.2. Catalyst characterization

UV–vis DR spectra of air-dried, as-prepared (calcined at 500 °C) and dehydrated at oxidizing condition *n*% Cu(α)ZSM-5 samples were obtained at room temperature using a Shimadzu UV-2501 PC spectrophotometer equipped with a diffuse reflectance accessory (ISR-240 A). The air-dried and as-prepared samples were used without their thermal pretreatment in situ, i.e. after exposition to ambient conditions. For dehydration at oxidizing condition, the sample (pellets of 0.1–0.25 mm) was placed into the special home-made UV–vis DR quartz cell and evacuated at room temperature to 0.1 mbar. Then 250 mbar of oxygen was added. After that temperature was increased to 400 °C, and the sample was calcined for 2 h. The water vapor was frozen in a trap at 70° C. After calcination, the sample was cooled in a closed oxygen atmosphere in order to eliminate ingress of moisture. For dehydration at vacuum condition, the sample was evacuated into the UV–vis DR cell at 400 °C for 2 h, after that 130 mbar of oxygen was added. The spectra were recorded against a $BaSO_4$ reflectance standard in the range of 900–190 nm (11,000–54,000 cm^{-1}). Below, the UV–vis DR spectra are shown in the Kubelka–Munk representation, $F(R_\infty)$.

ESR spectra of the samples were recorded on a Bruker EMX EPR spectrometer with microwave region l = 3 cm, high-frequency modulation of magnetic field 100 kHz, and magnetic field up to 5000 G at 100 and 295 K in a quartz glass ampoule with the internal diameter of 3 mm. Parameters of the ESR spectra were determined by a comparison with the spectrum of diphenylpicrylhydrazyl (DPPH, $g = 2.0037 \pm 0.0002$).

The temperature-programmed reduction experiments were conducted using a flow reactor connected with a thermal conductivity detector. A Cu-substituted ZSM-5 sample (100 mg, fraction 0.25–0.50 mm) was placed in the reactor, pretreated in the oxygen flow (30 cm^3/min) at 400 °C for 0.5 h and cooled to room temperature. Then, a hydrogen–argon mixture (10 vol.% H_2) was passed through the Cu–ZSM-5 sample as the reducing agent at a feed rate of 30 cm^3/min. The temperature range and heating rate were

25–630 °C and 10 °C/min, respectively. Water formed during the reduction of the copper–oxygen compounds was frozen out in a trap at −70 °C. The hydrogen consumption was calibrated against the reduction of CuO (Reachem, very-high-purity) under similar conditions, assuming a complete one-step CuO reduction to zero-valent copper.

The Cu–ZSM-5 catalysts were tested in selective catalytic NO reduction with propane (SCR NO–C_3H_8) in oxygen presence. Their catalytic activity was studied using the flow reactor. The compositions of the feed and reaction products were determined with a continuous analyzer TEST-1 equipped with electrochemical sensors; precision 5 ppm for NO, 5 ppm CO, 0.005 vol.% for C_3H_8 and 0.1 vol.% for O_2. The catalytic activity was measured in the temperature range 200–550 °C during both heating and cooling cycle with the gas flow rate 42,000 h^{-1}. The catalyst was used as 0.5–1.0 mm grains mixed with 1–2 mm quartz particles in a 1:1 ratio. The catalyst volume was 0.5 cm^3. The feed consisted of 340 ppm NO, 0.15 vol.% C_3H_8, 3.1–3.2 vol.% O_2 and Ar balance. The catalytic activity was characterized as NO and C_3H_8 conversions (X_{NO} and X_{CH}, %) at a desired temperature. For all studied *n*% Cu(α)ZSM-5 catalysts, a discrepancy within experimental error was observed for NO and C_3H_8 conversion measured during heating and cooling cycle.

The rate constant of NO conversion at 275 °C normalized per 1 g of the Cu–ZSM-5 catalyst (k_{NO}, $1/g_{Cat}$ s) were calculated according to Eq. (2) assuming that the reactor operated in the ideal plug flow mode and the NO reduction was the first order reaction:

$$k_{NO} = -\frac{\mathrm{Ln}(1 - X_{NO}/100)}{\tau \times m}(1/g_{Cat} \times s), \quad (2)$$

Here, X_{NO} is the NO conversion (%) at 275 °C, τ is the space time (s), *m* is the catalyst mass (g). The rate constant of propane conversion at 275 °C normalized per 1 g of the catalyst (k_{C3H8}, $1/g_{Cat}$ s) were calculated the same matter.

3. Results and discussion

3.1. State of copper ions in aqueous and water–ammonia solutions

The state of copper ions in aqueous solutions of copper salts is known to strongly depend on their concentration and pH of solution.

The dissolution of copper salts in water produces the hydrated ions - hexaaquacopper(II), $[Cu(H_2O)_6]^{2+}$; at certain pH values they can undergo electrolytic dissociation (the hydrolysis, reactions (1)–(3)) to form mono- and binuclear complexes of the Cu^{2+} cation, in particular $[Cu(H_2O)_5(OH)]^+$ and $[Cu_2(OH)_2(H_2O)_8]^{2+}$. The final product of the hydrolysis is copper hydroxide (Reaction (4)).

$$[Cu(H_2O)_6]^{2+} \rightarrow [Cu(OH)_j(H_2O)_{6-j}]^{2-j} + jH^+ (j = 1-4) \quad (1)$$

$$2[Cu(H_2O)_5(OH)]^+ \rightarrow [Cu_2(OH)_2(H_2O)_8]^{2+} + 2H_2O \quad (2)$$

$$2[Cu(H_2O)_6]^{2+} \Leftrightarrow [Cu_2(OH)_2(H_2O)_8]^{2+} + 2H^+ + 2H_2O \quad (3)$$

$$[Cu(H_2O)_5(OH)]^+ \rightarrow Cu(OH)_2\downarrow + H^+ + 4H_2O \quad (4)$$

At a concentration of 0.01–0.1 M, the hexaaquacopper(II) ion starts to hydrolyze at pH above 4 and can precipitate soon after that as a trihydrate of copper oxide or hydroxide [23]. The $[Cu(H_2O)_5(OH)]^+$ ion is unstable in aqueous solutions ($K_{11} < 10^{-8}$) [24] and tends to association, which leads to the formation of binuclear hydroxocomplex $[Cu_2(OH)_2(H_2O)_8]^{2+}$ by Reaction (2) [23,24]. Thus, even in the low concentrated solutions of copper salts (<0.001 M), the binuclear hydroxocomplexes are present along with $[Cu(H_2O)_5(OH)]^+$ [23,24]. In the concentrated solutions of copper salts (>10^{-3} M), copper ion is hydrolyzed mainly with the formation of hydroxocomplexes $[Cu_2(OH)_2(H_2O)_8]^{2+}$ by Reaction (3) [23].

It is assumed [23] that the binuclear complexes can be involved in polycondensation or the so-called "core-plus-links" reaction (Reactions (5) and (6)) to form polynuclear hydroxocomplexes $[Cu_n(OH)_{2n-2}(H_2O)_{4+2n}]^{2+}$ ($n \geq 3$).

(5) $[Cu(H_2O)_6]^{2+} + [Cu_2(OH)_2(H_2O)_8]^{2+} \rightarrow [Cu_3(OH)_4(H_2O)_{10}]^{2+} + 2H^+ + 2H_2O$

(6) $[Cu(H_2O)_6]^{2+} + [Cu_n(OH)_{2n-2}(H_2O)_{4n-2}]^{2+} \rightarrow [Cu_{n+1}(OH)_{2n}(H_2O)_{4n}]^{2+} + 2H^+ + 2H_2O$ ($n > 2$)

Thus, the occurrence of hydrolysis, association and polycondensation of hexaaquacopper(II) ions in solutions is responsible for the diversity of copper ion states in aqueous solutions. It defines often the characteristics of the zeolite ion exchange with aqueous solutions of copper salt. This diversity was examined in detail by Baes and Mesmer [24] for the concentration range of 10^{-5}–0.1 M, which is used most often for the synthesis of Cu-substituted zeolites. For example, it was shown that in the 0.1 M solutions of copper salts with pH < 5 the hexaaquacopper(II) complex is predominant; at pH close to 6, comparable amounts of $[Cu(H_2O)_6]^{2+}$ and $[Cu_2(OH)_2(H_2O)_8]^{2+}$ complexes are present in the solutions; and at pH > 11, the negatively charged complexes $[Cu(OH)_3(H_2O)_3]^-$ and $[Cu(OH)_4(H_2O)_2]^{2-}$ are formed in addition to $[Cu_2(OH)_2(H_2O)_8]^{2+}$. Note that in the pH range of 5–10 the $[Cu(H_2O)_5(OH)]^+$ ion is absent in the concentrated solutions; so, it cannot participate in the ion exchange. While content of $[Cu_2(OH)_2(H_2O)_8]^{2+}$ in copper acetate solutions can reach 20–50% [24], which leads to the well-known increase in the Cu-exchange level at the Cu–ZSM-5 preparation.

In the low-concentrated copper solutions (10^{-5}–10^{-3} M), the $[Cu(H_2O)_6]^{2+}$ complex is virtually not hydrolyzed up to pH close to 6, the hydrolysis products of copper cation being formed in comparable amounts at pH 7–11. For example, the $[Cu(H_2O)_6]^{2+}$, $[Cu(H_2O)_5OH]^+$ and $[Cu_2(OH)_2(H_2O)_8]^{2+}$ complexes coexist at pH 7–8.5, while at pH 9–11 there appears a substantial amount of $Cu(OH)_2$ precipitate, which completely dissolves only in the strongly alkaline solutions with pH > 12 [24].

The water–ammonia copper salt solutions have a more complicated composition of copper complexes. After the addition of ammonia solution to the aqueous copper acetate solution, precipitation of copper hydroxide is observed, which is followed by its dissolution with the formation of ammonia–copper complexes $[Cu(NH_3)_n(H_2O)_{6-n}]^{2+}$ (so-called Schweitzer's reagent). The composition of ammonia–copper complexes depends on the NH_4^+/Cu^{2+} ratio and pH of the medium. The NH_3 amount increases with raising the pH and NH_4^+/Cu^{2+} ratio; this provokes consecutive substitution of H_2O and OH^- ligands in the coordination sphere of Cu^{2+} ion by ammonia ligands. Thus, the $[Cu(NH_3)_3(H_2O)_3]^{2+}$ and $[Cu(NH_3)_4(H_2O)_2]^{2+}$ complexes are predominant at pH 7–8 and 8.5–10.5, respectively; at pH > 10 the $[Cu(NH_3)_4(H_2O)_2]^{2+}$ is coexisted with $[Cu(NH_3)_5(H_2O)_2]^{2+}$ complex [25,26]. Note that among copper ammine complexes most stable is the $[Cu(NH_3)_4]^{2+}$ complex ($\beta_2 = 7.9 \times 10^{12}$). It cannot be ruled out that at a low ammonia concentration ($NH_4^+/Cu^{2+} < 4$) in the solution not only the ammonia–copper complexes are present but also the $[Cu(H_2O)_5(OH)]^+$, $[Cu_2(OH)_2(H_2O)_8]^{2+}$ and polynuclear hydroxocomplexes. After the formation of tetraammine complex at NH_4^+/Cu^{2+} near 6–15 the concentration of Cu^{2+} ions is quite low and insufficient for attaining the product of copper(II) hydroxide solubility equal to 5.6×10^{-20}. On the other hand, in a strongly alkaline medium ($NH_4^+/Cu^{2+} > 20$, pH > 12.5) the formation of CuO is possible due to a decreased stability of soluble ammonia copper complexes [25]. In addition, the high ammonia concentrations can cause desilication of the zeolite surface, which is desirable to avoid. This is why the ion exchange is necessary performed using the ammonia solutions of copper salts with pH 10.0–11.0.

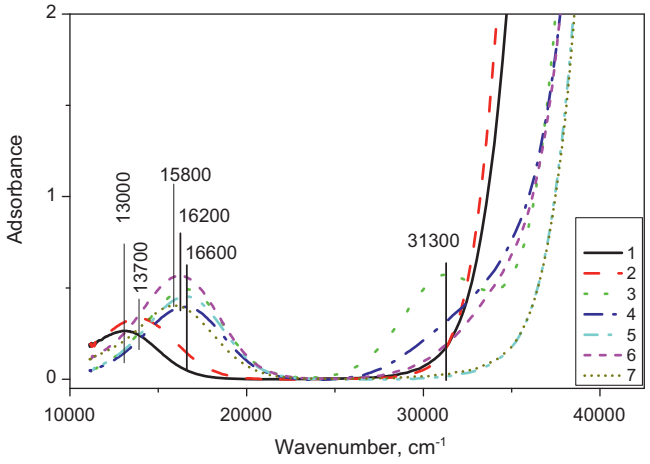

Fig. 1. Electronic spectra of copper acetate solutions with the copper concentration of 6 g/l: aqueous (curves 1 and 2) and water–ammonia solutions with a NH_4^+/Cu^{2+} ratio equal to 3 (curve 3), 6 (curves 4 and 5), 15 (curve 6), and 30 (curve 7). Spectra of aqueous (curve 2) and water–ammonia (curve 5) solutions of copper acetate with NH_4CH_3COO (77 g/l), which was added to increase the ionic force of solutions and suppress the hydrolysis of hexaaquacopper(II) complexes, are presented for comparison.

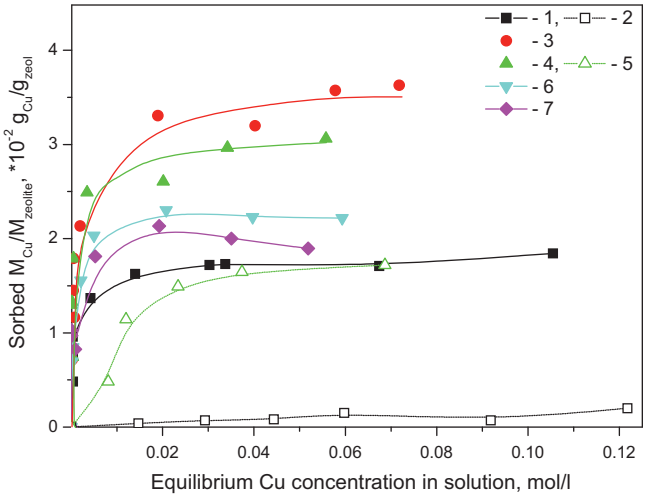

Fig. 2. Curves for the sorption of copper cation from aqueous and water-ammonia copper acetate solutions by H–ZSM-5–17 zeolite at a NH_4^+/Cu^{2+} ratio equal to 0 (1,2), 3 (3), 6 (4,5), 15 (6), and 30 (7). Sorption curves (2,5) obtained for the aqueous and water–ammonia copper acetate solutions with addition of 77 g/l NH_4CH_3COO is presented for comparison. Data on the copper content in Cu–ZSM-5 were obtained by ICP AES.

The electronic absorption spectra of aqueous and water–ammonia copper acetate solutions (Fig. 1) correlate with the literature data. For example, an aqueous solution of copper acetate (6 g Cu/l) is characterized by the absorption band at 13000 cm^{-1} (Fig. 1, curve 1) corresponding to the d–d transition of isolated Cu^{2+} ions in a tetragonally distorted octahedral coordination of the water ligands [27]. The addition of ammonium acetate (77 g/l) to the copper acetate solution shifts the a.b. to 13,700 cm^{-1} (Fig. 1, curve 2). The observed energy shift of the d–d transition of isolated Cu^{2+} ions indicates that water ligands in its coordination sphere are partially substituted by ammonia ligands [28]. In the near UV region, the spectra of aqueous copper acetate solutions with and without ammonium acetate were identical.

In the absorption spectra of water–ammonia copper acetate solutions with the molar concentration ratio NH_4^+/Cu^{2+} of 3–6, the band at 16,600 cm^{-1} is observed (Fig. 1, curves 3 and 4), which corresponds to the d–d transitions in tetraammine copper complexes [28], $[Cu(NH_3)_4]^{2+}$. As the concentration ratio NH_4^+/Cu^{2+} increases to 15 and 30 (Fig. 1, curves 6 and 7), energy of the d–d transition shifts to the region of 16,200 and 15,800 cm^{-1}, respectively. The observed energy shift of the d–d transition corresponds to the formation of pentaammine copper complexes [28], $[Cu(NH_3)_5]^{2+}$.

In distinction to aqueous copper acetate solutions, spectra of the water–ammonia copper acetate solutions show the absorption in the region of 31,300 cm^{-1}. The absorption intensity in this region decreases with increasing the ammonia concentration in a solution, which shows up as a growth of the NH_4^+/Cu^{2+} ratio from 3 to 30 (Fig. 1, curves 3,4,6,7). The indicated band is virtually symmetrical for a solution with the concentration ratio $NH_4^+/Cu^{2+} = 3$ (Fig. 1, curve 3). This solution had a low stability: a black substance precipitated from the solution for 24 hours. According to electron microscopy data, the composition of this precipitate corresponded to CuO^*3H_2O. Absorption in the region of 31,300 cm^{-1} is completely absent in the absorption spectra of water–ammonia copper acetate solutions with $NH_4^+/Cu^{2+} = 30$ (Fig. 1, curve 7). The indicated facts give grounds to consider the band at 31,300 cm^{-1} as the ligand–metal charge transfer band (CTB L-M) in the copper structures with a square-planar coordination of the oxygen-containing [4,27] and/or hydroxyl-containing ligands. The formation of square-planar copper oxide/hydroxide complexes is related to the hydrolysis of hexaaquacopper(II) complexes (Reactions (2)–(4)). Note that ammonium acetate added to the water–ammonia copper acetate solution in the amount corresponding to 1 M solution naturally hinders the hydrolysis of hexaaquacopper(II) complexes. As a result, absorption in the region of 31,300 cm^{-1} completely disappears from the spectrum of water–ammonia copper acetate solution (Fig. 1, compare curves 4 and 5), while energy of the d–d transition of tetraammine complex does not change.

Similar trends are observed also in the absorption spectra of diluted aqueous and water–ammonia copper acetate solutions with the copper concentration of 1 g/l.

Naturally, the composition of copper ions in aqueous solutions affects the regularities of the ion exchange in H–ZSM-5 zeolite; in particular, it exerts an effect on the sorption capacity and state of copper cations stabilized in the zeolite. In its turn, this produces differences in the RedOx properties of Cu-substituted ZSM-5 zeolites and their $DeNO_x$ reactivity.

3.2. *Sorption isotherms of Cu^{2+} ions from aqueous and ammonia solutions of copper acetate*

Fig. 2 displays the isotherms of copper cations sorption by H–ZSM-5 zeolite from aqueous and water–ammonia copper acetate solutions upon variation of the concentration ratio NH_4^+/Cu^{2+} in the range of 0–30. In the case of ion exchange with aqueous copper acetate solutions (having pH close to 5.7–6.0), the amount of copper sorbed by the zeolite increases with its concentration in solution (Fig. 2, curve 1). The maximum amount equal to 2 wt.% Cu was attained at a copper concentration in initial solution of 2.5 g/l (or 0.04 mol/l) and above. The indicated copper content in Cu–ZSM-5 corresponded to a 80% exchange of the zeolite protons for the copper cations ($Cu/Al_{at} = 0.4$) under the assumption that the ion exchange proceeds by Reaction (8) (Table 1) and its stoichiometry corresponds to the exchange of $2H^+$ of zeolite for one Cu^{2+} cation.

The addition of ammonia to the aqueous copper acetate solutions (Fig. 2, curves 3–7) produced a nonlinear effect on the copper content in Cu-substituted ZSM-5 catalysts synthesized with such solutions. For example, at a molar concentration ratio NH_4^+/Cu^{2+} less than 6, the copper content of Cu–ZSM-5 increases substantially in comparison with the sample synthesized with aqueous copper

Table 1
Main reactions occurring at the ion exchange of H–ZSM-5 with aqueous and water–ammonia solutions of copper acetate.

Molar ratio NH_4^+/Cu^{2+}	Composition of copper complexes in solution	Main ($\alpha = 0$) and concurrent ($\alpha = >0$) reactions affecting the level of Cu exchange	Cu/Al
$\alpha = 0$	$[Cu(H_2O)_6]^{2+}$	$\equiv$Z-OH → [$\equiv$Z-O$^-$] + H$^+$ (7) $2\equiv Z\text{-}O^- + [Cu(H_2O)_6]^{2+}_{aq} \leftrightarrow \{Cu(H_2O)_6\}^{2+}\text{-}[^-O\text{–}Z\equiv]_2$ (8)	= 0.5
$\alpha < 6$	Large $Cu_x(OH)_y$	$\equiv$Z-OH → [$\equiv$Z-O$^-$] + H$^+$ (7) $2\equiv Z\text{-}O^- + [Cu(NH_3)_4]^{2+}_{aq} \leftrightarrow \{Cu(NH_3)_4\}^{2+}\text{-}[^-O\text{-}Z\equiv]_2$ (9) $[Cu(H_2O)_5(OH)]^+ \rightarrow Cu(OH)_2\downarrow + H^+ + 4H_2O$ (4) $[Cu_{aq}]^{2+} + [Cu_n(OH)_{2n-2}]^{2+}_{aq} \rightarrow [Cu_{n+1}(OH)_{2n}]^{2+}_{aq} + 2H_{aq}^+$ (6)	> 0.5
$\alpha = 6$–15	$[Cu(NH_3)_4(H_2O)_2]^{2+}$, $[Cu_2(OH)_2]^{2+}$	$\equiv$Z-OH → [$\equiv$Z-O$^-$] + H$^+$ (7) $2\equiv Z\text{-}O^- + [Cu(NH_3)_4]^{2+}_{aq} \leftrightarrow \{Cu(NH_3)_4\}^{2+}\text{-}[^-O\text{-}Z\equiv]_2$ (9) $\equiv Z\text{-}O^- + [Cu_2(OH)_2]^{2+}_{aq} \rightarrow Cu(OH)^+\text{-}[^-O\text{-}Z\equiv] + [CuOH]^+_{aq}$ (10) $\equiv ZO^-\text{-}Cu(OH)^+ + [Cu_2(OH)_2]^{2+}_{aq} \rightarrow \{Cu_2(OH)_3\}^+\text{-}[^-O\text{-}Z\equiv] + + [CuOH]^+_{aq}$ (11)	> 0.5
$\alpha = 30$	$[Cu(NH_3)_4(H_2O)_2]^{2+}$	$2\equiv Z\text{-}O^- + [Cu(NH_3)_4]^{2+}_{aq} \leftrightarrow \{Cu(NH_3)_4\}^{2+}\text{-}[^-O\text{-}Z\equiv]_2$ (9) $\equiv Z\text{-}OH + NH_4^+ \rightarrow \equiv Z\text{-}ONH_4 + H^+$ (12) $\text{-}Si\text{-}O^- + [Cu(NH_3)_4]^{2+}_{aq} \leftrightarrow \{Cu(NH_3)_4\}^{2+}\text{-}[^-OSi]_2$ (13)	< 0.4

$\equiv$Z-OH – cation exchange site Si(OH)Al of H-ZSM-5 zeolite.

acetate solutions. Note that this regularity was observed over the entire range of copper acetate concentrations in the ion-exchange solution; therewith, a maximum copper content in Cu–ZSM-5 was as high as 3.2–3.8 wt.% (Fig. 2, curve 3). An excess of copper content over the stoichiometric value (Cu/Al_{at} = 0.65–0.80 instead of 0.5) is caused by the hydrolysis and polycondensation of hydrated copper ions (Reactions (4), (5) and (6), which proceed in aqueous copper salt solutions at pH 8–9 with the formation of large copper polyhydroxocomplexes (CTB L-M at 31,300 cm^{-1}, Fig. 1, curve 3). However, due to their big size, such complexes cannot enter the zeolite channels; so, they may precipitate on the external surface of the zeolite crystallites.

When the NH_4^+/Cu^{2+} ratio is varied within 6–15, the amount of copper sorbed by the zeolite decreases to 2.3–2.8 wt.% (Fig. 2, curves 4,6), which corresponds to the Cu/Al_{at} values in the range of 0.50–0.60. In this case, the formation of over-exchanged Cu–ZSM-5 catalysts is related to both the tetra-, pentaammine copper complexes (d–d transition at 16,200–16600 cm^{-1}) and binuclear copper complexes $[Cu_2(OH)_2]^{2+}$ (CTB L-M at 31,300 cm^{-1}, Fig. 1, curves 4,6) involved in the ion exchange. The latter ones, as was discussed above, appear in the solutions with pH 7–10.5 due to Reactions (2) and (3). The main ion exchange reactions can be represented in this case by the equations of Reactions (9) and (10) (Table 1). One cannot rule out that the mononuclear complex $[Cu(OH)]^+$ is also involved in the ion exchange in the low-concentrated water–ammonia copper acetate solutions, although its concentration in ammonia solutions should be negligibly low due to occurrence of association and ammonia–complexation processes.

A further increase in the concentration ratio NH_4^+/Cu^{2+} to 30 (pH 11.5) is accompanied by a decrease in the copper content of Cu–ZSM-5 to 1.85–2 wt.% (Fig. 2, curve 7), which corresponds to a level of Cu exchange below 100% (Cu/Al_{at} < 0.5). It should be noted that only in the case of ion exchange in strongly alkaline media, the amount of copper sorbed by H–ZSM-5 zeolite showed a weak tendency to decrease with increasing the copper concentration in initial solution. The observed tendency can be attributed to concurrent ion exchange reactions of the zeolite protons with copper–ammonia and NH_4^+ ions (Reactions (9) and (12), Table 1).

Note that during the ion exchange between a proton compensating for the charge of zeolite lattice and a hydrated copper cation, in both the aqueous and water–ammonia suspensions, the H^+ ions are released into solution, which leads to its acidification. So, the composition of copper complexes may change in the course of ion exchange. It is possible also that binuclear and polynuclear copper hydroxocomplexes may form in the zeolite channel due to local changes of pH during the ion exchange. To exclude the effect of such changes and prevent the hydrolysis of copper cations, 77 g/l (1 M) of ammonium acetate was added to aqueous and water–ammonia copper acetate solutions. We noticed that pH changed only slightly during the ion exchange: even in water–ammonia solutions with the copper concentration of 1 g/l, such changes did not exceed 0.9 pH units (Table 2, example 9). As seen from Fig. 2, after the addition of ammonium acetate to water–ammonia copper acetate solutions with the concentration ratio NH_4^+/Cu^{2+} equal to 6 (Fig. 2, curve 5), the amount of sorbed copper decreased virtually twofold over the entire range of copper concentrations in solution, and its maximum amount did not exceed 1.6 wt.% (Cu/Al_{at} = 0.33). The increasing of ammonium acetate concentration in this solution up to 231 g/l (3 M) resulted in a further decline in copper loading in Cu–ZSM-5, its maximum content amounted to 1 wt.% (Cu/Al_{at} = 0.2). But in the case of aqueous solution of copper acetate, the addition of 77 g/l of NH_4CH_3COO led to the decrease of ion exchange between zeolite proton and Cu^{2+} ions by more than 90% (Fig. 2, curve 2). The unlike effect of ammonium acetate adding on the saturation Cu content is most likely due to different extent of zeolite dissociation occurring in water and water–ammonia solutions in accordance with Reaction (7). A very weak change of pH value or no change, which was observed during the ion exchange with the aqueous solution of copper acetate in presence of NH_4CH_3COO adding (Table 2, example 8), illustrates extremely low extent of the zeolite dissociation. The last is the reason of a slow ion exchange between undissociated zeolite and hydrated copper(II) ions. In the case of the water-ammonia solution of copper acetate, the decrease of Cu-saturation content at ammonium acetate adding is related to a inhibition of hydrolysis of hexaaquacopper(II) ions as well as a competition between Cu^{2+} and NH_4^+ under ion-exchange conditions.

Treatment of the obtained copper ion sorption isotherms using various models showed that the ion exchange of H–ZSM-5 with aqueous and water–ammonia copper acetate solutions is adequately described within the Langmuir monomolecular adsorption theory. Table 2 lists the calculated amounts of copper, which are sorbed during the ion exchange of H–ZSM-5 zeolite with copper acetate solutions, and the adsorption equilibrium constants in dependence on the ion exchange conditions. During the ion exchange, an increase in the copper salt concentration in the solution naturally increased its content in the zeolite; however, a maximum amount of the sorbed copper is limited by the number of cation exchange sites (mainly acid groups Si(OH)Al, 600 ± 25 mkmol/g), the dynamic adsorption equilibrium, and the presence of competing cations capable of exchanging with the cation exchange sites of the zeolite (for example, NH_4^+, $[Cu_2(OH)_2]^{2+}_{aq}$). Furthermore we note that the maximum copper amount adsorbed from aqueous copper acetate solutions by H-form of ZSM-5 is a half times higher compared to its Na^+ and NH_4^+-forms (275 and 190–200 mkmol Cu/g, respectively, Table 2). The much lower saturation of Cu content upon exchange into the Na^+

Table 2
Amount of copper sorbed during the ion exchange of ZSM-5 zeolite (Si/Al = 17) with copper acetate solutions, and adsorption equilibrium constant versus the ion exchange conditions.

No.	Cationic form of zeolite	Conditions of exchange			A_{max}, μmol/g	k_s, l/mol
		NH_4^+/Cu^{2+}, α	pH^1	pH^2		
1	Na^+	0	5.8/5.4	5.5/5.4	200	960
2	NH_4^+	0	5.8/5.4	5.1/5.3	190	390
3	H^+	0	5.8/5.4	3.9/5.0	275	910
4	H^+	3	9.7/10.2	8.9/8.9	595	1055
5	H^+	6	10.5/10.7	9.7/10.2	475	2240
6	H^+	15	11.1/11.9	10.0/11.2	345	1800
7	H^+	30	11.6/12.1	10.3/11.5	310	2890
8	H^+	0+1 M NH_4Ac	6.5/5.8	6.0/5.8	29	19
9	H^+	6+1 M NH_4Ac	8.7/9.4	7.8/9.1	275	190

pH^1 is a pH value of the initial copper acetate solution with 1 g/l and 6 g/l copper concentration, respectively, used for the ion-exchange mode with zeolite.
pH^2 is a pH value of the spent copper acetate solution with 1 g/l and 6 g/l copper concentration, respectively, after the ion-exchange mode with zeolite.

or NH_4^+-form instead of H–ZSM-5 is due to their unequal dissociation degree in water. During the ion exchange, the H^+, Na^+ or NH_4^+ ions are released into solution, resulting in its acidification or alkalization, respectively. Alkalization of the solution leads to a shift of the reaction equilibrium to the left and accumulation of not dissociated zeolite form, and therefore to the smaller achievable Cu-exchange level.

It seems interesting to examine the effect of ion exchange conditions on the adsorption equilibrium constant, which is a ratio of rate constants for the adsorption and desorption of hydrated copper cations on the zeolite surface. A growth of the concentration ratio NH_4^+/Cu^{2+} from 0 to 6 is accompanied by a proportional increase in the adsorption equilibrium constant, at $NH_4^+/Cu^{2+} = 15$ this constant slightly decreases and starts to increase again at $NH_4^+/Cu^{2+} = 30$. Changes in the k_s value correlate with pH of aqueous and water–ammonia suspensions of H–ZSM-5 zeolite, which is caused by electrolytic dissociation of the zeolite proton sites. This gives grounds to assume that the ion exchange with aqueous and water–ammonia copper acetate solutions having a concentration ratio NH_4^+/Cu^{2+} of 0–15 involves mostly the acid bridging groups of the zeolite in a deprotonated or protonated state, Si(O^-)Al and Si(OH)Al. Whereas in a strongly alkaline medium, which is typical of water–ammonia copper acetate solutions with $NH_4^+/Cu^{2+} = 30$, the ion exchange involves not only the bridging Si(OH)Al groups but also the terminal silanol groups SiOH (about 40 mkmol/g). The terminal SiOH groups are deprotonated in strongly alkaline media and become negatively charged, thus acquiring the cation exchange ability [12,29]. This reaction has been thoroughly investigated for silica [30]. The involvement of SiOH groups in the ion exchange is undesirable because their interaction leads to localization of copper cations on the surface of zeolite crystallites. Upon heat treatment in the oxidizing medium, the $[Cu(NH_3)_4]^{2+}$ cations are transformed into CuO due to weak interaction with the SiOH groups [12,29].

3.3. State of copper ions in calcined Cu–ZSM-5 catalysts

Chemistry of the processes underlying the observed regularities of the copper cations sorption by H–ZSM-5 from aqueous and water–ammonia solutions agrees well with the data on the electronic state of copper cations in the as-prepared Cu–ZSM-5 catalysts and their evolution during heat treatment. Fig. 3 shows ESR spectra of *n*% Cu(α)ZSM-5 samples synthesized by the ion exchange with aqueous and water–ammonia solution of copper acetate with different NH_4^+/Cu^{2+} ratio.

The ESR spectra of the air-dried *n*% Cu(α)ZSM-5 samples with low and high Cu loading at 77 K contain the signal which parameters correspond to isolated hexaaquacopper(II) [4,14,16] and tetraamminecopper [9,30] complexes (Fig. 3A, curves 1 and 3–5, respectively). With increase of NH_4^+/Cu^{2+} ratio from 0 to 30, their ESR parameters change from $g_{||} = 2.38$, $A_{||} = 138$ G, $g_\perp = 2.08$ to $g_{||} = 2.24$, $A_{||} = 175$ G, $g_\perp = 2.03$. In ESR spectra of the calcined *n*% Cu(α)ZSM-5 samples (after contact with air, Fig. 3B), the isolated Cu^{2+} ions with ESR parameters $g_{||} = 2.38$, $A_{||} = 138$ G, $g_\perp = 2.08$ (type I) corresponding to their tetragonally distorted octahedral environment of oxygen-containing ligands are observed. These ions are located in cation-exchange positions of the zeolite.

The second type of the isolated Cu^{2+} ions with ESR parameters $g_{||} = 2.32$, $A_{||} = 165$ G, $g_\perp = 2.06$ (Fig. 3B type II) was recorded also in spectra of *n*% Cu(30)ZSM-5 samples prepared at $NH_4^+/Cu^{2+} = 30$. Their ESR parameters show that the tetragonal distortion of octahedral coordination of Cu^{2+} ions is bigger in comparison with the isolated Cu^{2+} ions of type I. These ions seem to be stabilized on a terminal SiOH-groups of the zeolite. This stabilization is usually observed for CuO/SiO_2 catalysts prepared by sorption of copper ions from copper–ammonia solutions [30].

The fraction of the ESR-visible isolated Cu^{2+} ions in *n*% Cu(α)ZSM-5 increases with NH_4^+/Cu^{2+} ratio from 3 to 30. Their quantity also increases when the samples were prepared from copper–ammonia solution with ammonium acetate additives suppressing hydrolysis of hexaaquacopper(II) complex.

Structures of Cu^{2+} ions with extra-lattice oxygen are ESR-silent owing to the strong exchange interaction between copper ions. They were studied by UV–vis electronic spectroscopy of diffuse reflectance. Fig. 4 displays the diffuse reflectance electronic spectra for the air-dried and calcined Cu–ZSM-5 samples.

The spectra of the dried and as-prepared Cu-substituted ZSM-5 catalysts synthesized with aqueous copper acetate solution show the absorption bands at 12,200 and 47,500 cm^{-1} (Fig. 4A and B, curves 1). Energies of these bands correspond to the energy of d–d transition and ligand–metal charge transfer band, respectively, of the isolated copper ions in a tetragonally distorted octahedral coordination of the oxygen-containing and/or water ligands ($Cu^{2+}{}_{Oh}$) [27]. These ions are close to hexaaquacopper(II) complex by the energy of d–d transition. The hexahydrated copper(II) ions are present in the calcined Cu–ZSM-5 samples because the sample has been exposed at ambient conditions and adsorbed ambient humidity. The isolated $Cu^{2+}{}_{Oh}$ ions are stabilized in the cation exchange positions of the hydrated and partially dehydrated zeolite ZSM-5 and were observed earlier in zeolites of various structural types: ZSM-5 [4,31,32], BEA [33], SSZ-13 [34] and others. For 2% Cu(0)ZSM-5 sample, the fundamental absorption edge (FAE) is observed in the UV region of the spectrum at 35,000 cm^{-1} (Fig. 4B, curve 7). FAE is caused by the band gap of the zeolite [4], which is typical of dielectric oxide structures.

The isolated $Cu^{2+}{}_{Oh}$ ions having d–d transition at 12,200 cm^{-1} remain also as one of the electronic states in the as-prepared

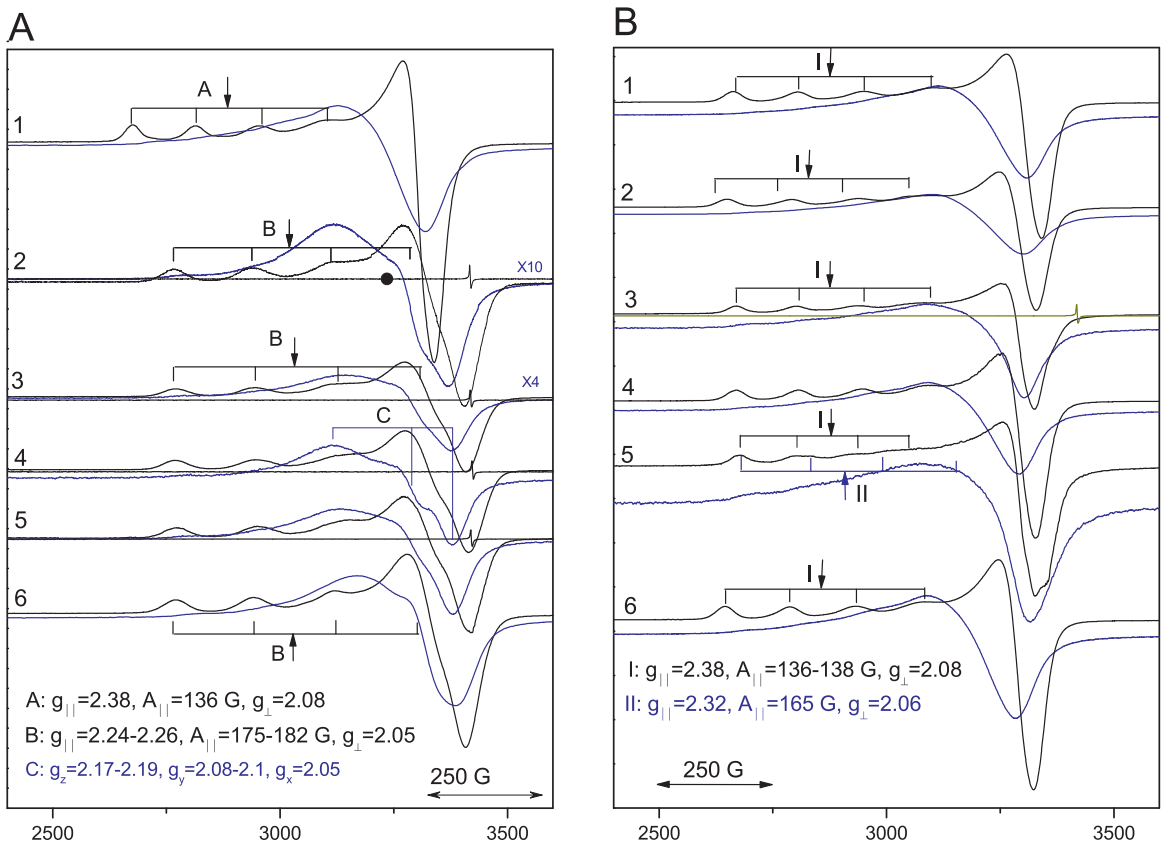

Fig. 3. ESR spectra of the air-dried (A) and calcined (B) *n*% Cu(α)ZSM-5-x samples prepared at a NH_4^+/Cu^{2+} ratio equal to 0 (2 wt.% Cu, Cu/Al = 0.4, curve 1), 3 (3.5 wt.% Cu, Cu/Al = 0.68, curve 2), 6 (2.9 wt.% Cu, Cu/Al = 0.57, curve 3), 15 (2.2 wt.% Cu, Cu/Al = 0.43, curve 4) and 30 (1.85 wt.% Cu, Cu/Al = 0.36, curve 5). ESR spectra of 1.7% Cu(6*)ZSM-5–0.33 prepared from water–ammonia copper acetate solution with NH_4CH_3COO (77 g/l, curve 6) are presented for comparison. Spectra were registered at 100 K (black, with hyperfine structure around $g_{||}$) and 295 K (blue).

Cu-substituted ZSM-5 catalysts synthesized with water–ammonia copper acetate solutions at a concentration ratio NH_4^+/Cu^{2+} of 3–30 (Fig. 4B, curves 2–5). However, they are formed during thermal treatment of the air-dried Cu–ZSM-5 samples from isolated ammine complexes of copper(II), having an energy of d–d transition at 14,600–15,600 cm^{-1} and CTB L–M at 45,000 cm^{-1} of UV–vis DR spectra (Fig. 4A, curves 2–5), instead of hexaaquacopper(II) ions (Fig. 4A, curve 1) as it was in the case of aqueous solutions of copper acetate. The shift of a.b. from 16,600 cm^{-1} typical of the tetraammonia-copper complex in water–ammonia solutions [27] (Fig. 2, curves 3–5) to 14,600–15600 cm^{-1} observed in UV–vis DR spectra of our ex-ammonia–copper 3.5% Cu(3)ZSM-5–0.68 and 2.9% Cu(6)ZSM-5–0.57 catalysts (Fig. 4) indicates that the copper–ammonia complex is anchored on the zeolite cation-exchange site and contains a less number of ammonia ligands compared with tetraammonia–copper complex.

In addition to a.b. 12,200 cm^{-1}, a weak absorption in the region of 32,500 and 37,500 cm^{-1} are observed also in the UV–vis DR spectra of the as-prepared ex-ammonia–copper *n*% Cu(α)ZSM-5 catalysts. The intensity of these absorption bands, which show up as the shoulders against FAE, increases with lowering the NH_4^+/Cu^{2+} ratio in the ion-exchange solution and reaches its maximum value at NH_4^+/Cu^{2+} = 3 (Fig. 4B, curve 2). These bands may be related to CTB L–M in the square-planar copper oxide clusters [4] and the weakly bound magnetic associates of $Cu^{2+}{}_{Oh}$ cations [8], respectively. The both structures have extra-lattice oxygen and are formed from mono-, bi- and polynuclear copper hydroxocomplexes (absorption at 31,000–33500 cm^{-1}, Fig. 4A, curves 2,3) during heat treatment of the air-dried ex-ammonia–copper Cu–ZSM-5 catalysts in the oxygen-containing medium. Note that the absorption around 32,500 and 37,500 cm^{-1} by Cu–ZSM-5 catalysts significantly decreased at high ammonia concentrations (for example, at NH_4^+/Cu^{2+} = 30, Fig. 4, curves 5) as well as at the addition of ammonium acetate to copper–ammonia solutions with NH_4^+/Cu^{2+} = 6 (Fig. 4, curves 6). As it was discussed above, the reasons for this are copper–ammonia complexation and suppression of hydrolysis of hexaaquacopper(II) ions, respectively.

The UV–vis DR spectra of the as-prepared samples synthesized at a low concentration of ammonia (NH_4^+/Cu^{2+} = 3) have two distinctive features: an intense absorption in the visible region of the spectrum at 13,500–14300 cm^{-1} and an increased absorption background (Fig. 4B, curve 2). The absorption is caused by the fundamental absorption edge of copper oxide; however, its position is somewhat shifted from the value typical of the bulk copper oxide (11,000 cm^{-1}). As the copper content in *n*% Cu(3)ZSM-5 increases from 1.0 to 3.5 wt.%, FAE of CuO particles shows a weak tendency to shift from 14,300 to 13,500 cm^{-1}. In the process, the band gap width changes from 3.70 to 4.25 eV (Fig. 5), thus indicating an increase in number of the defect of CuO nanoparticles. Such particles are produced by decomposition of large copper polyhydroxocomplexes located on the external surface of the air-dried Cu–ZSM-5 zeolite during its calcination.

Further formation of catalytically active copper structures in Cu–ZSM-5 is usually associated with dehydration of the samples [3,32,35]. Dehydration of our *n*% Cu(α)ZSM-5 samples in oxidizing condition at 400 °C (without water traces) results in a change of the coordinated environment of the isolated Cu^{2+} ions. Shift of d–d transition band from 12,200 to 13,500 cm^{-1}, an increase of its width and intensity as well as shift of CT L–M band from 47,500 to 44,700 cm^{-1} (Fig. 4C, curves 1, 4–6) point to a strong increase of

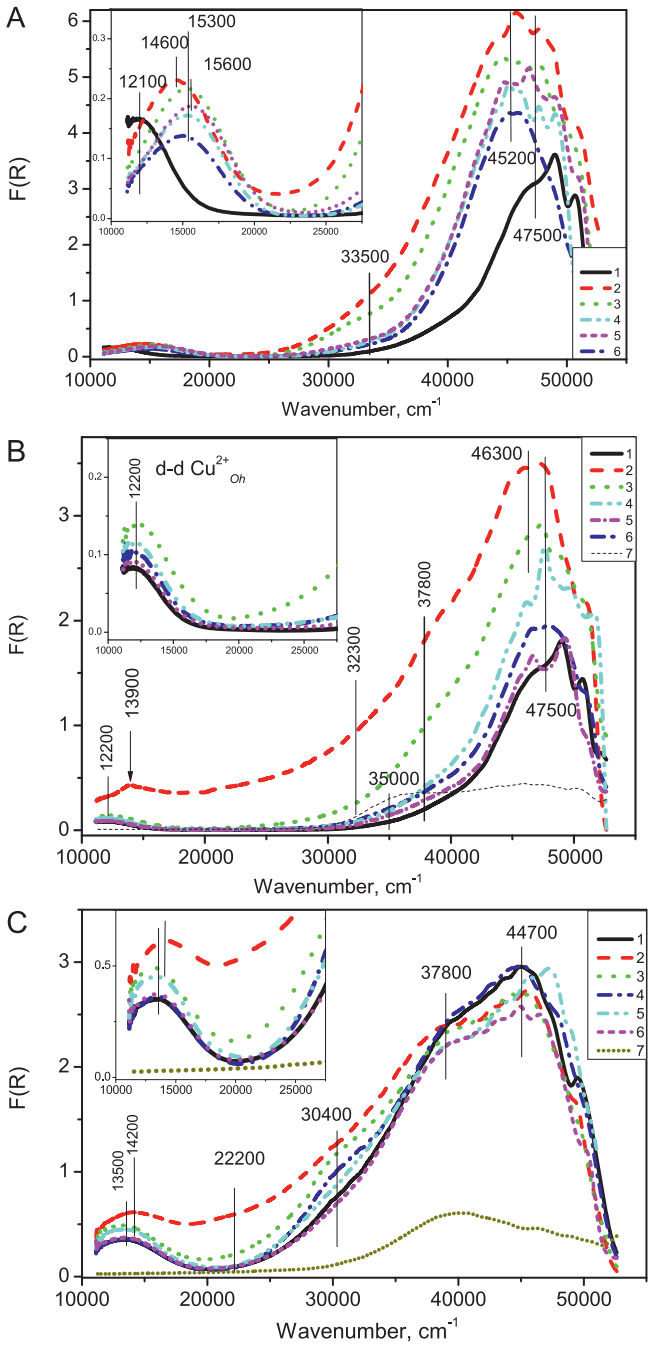

Fig. 4. UV–vis DR spectra of the air-dried (A), calcined at 500 °C and exposed to ambient conditions (B), dehydrated at oxidizing condition in UV–vis DR cell at 400 °C (C) *n*% Cu(*α*)ZSM-5-x samples prepared at a NH_4^+/Cu^{2+} ratio equal to 0 (2 wt.% Cu, Cu/Al = 0.4, curve 1), 3 (3.5 wt.% Cu, Cu/Al = 0.68, curve 2), 6 (2.9 wt.% Cu, Cu/Al = 0.57, curve 3), 15 (2.2 wt.% Cu, Cu/Al = 0.43, curve 4) and 30 (1.85 wt.% Cu, Cu/Al = 0.36, curve 5). UV–vis DR spectra of 1.7% Cu(6*)ZSM-5–0.33 prepared from water–ammonia copper acetate solution with NH_4CH_3COO (77 g/l, curve 6) and H–ZSM-5 (curve 7) are presented for comparison.

tetragonal symmetry of isolated Cu^{2+} ions. The UV–vis DR spectra of the dehydrated 3.5% Cu(3)ZSM-5–0.68 and 2.9% Cu(6)ZSM-5–0.57 samples (Fig. 4C, curves 2 and 3) are characterized by the stronger shift of d–d transition band (to 14,200 cm^{-1}) and its asymmetry as well as an increased absorption background in comparison with samples prepared at NH_4^+/Cu^{2+} ratio higher than 6. The two former features testify to heterogeneity of isolated Cu^{2+} ions. The latter indicates a formation of copper oxide nanoparticles.

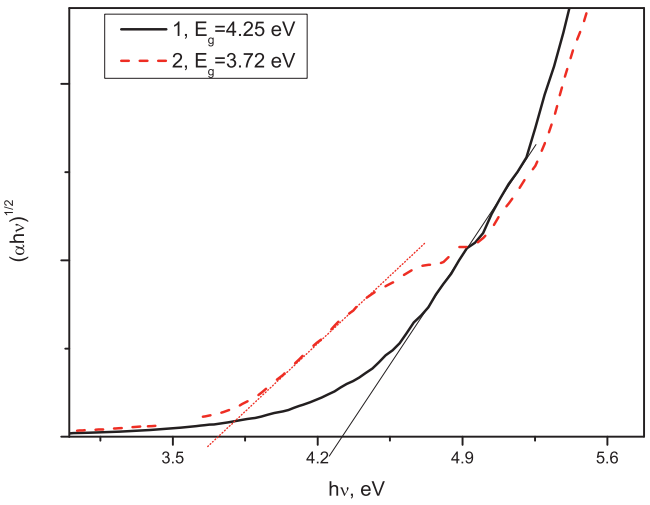

Fig. 5. The α-absorption plot for 3.5% Cu(3)-ZSM-5–0.68 (curve 1) and 0.7% Cu(3)–ZSM-5 (curve 2) catalysts.

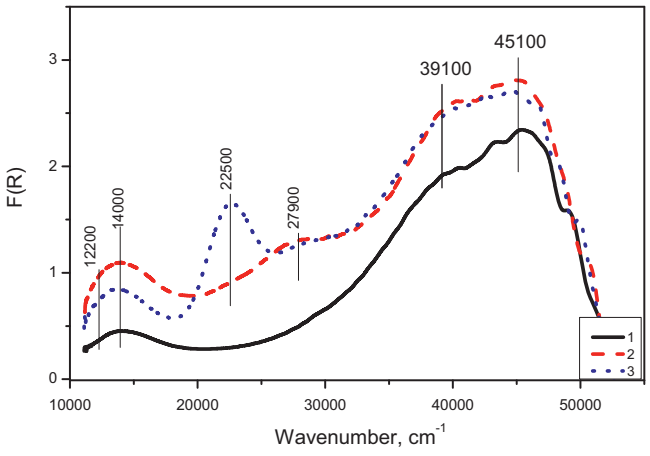

Fig. 6. UV–vis DR spectra of the 2.9% Cu(6)ZSM-5–0.57 sample dehydrated at oxidizing condition (curve 1), the sample after vacuum treatment (curve 2) and the latter after subsequent oxidizing (curve 3). Temperature of pretreatment was 400° C.

In addition to a.b. 13,500–14200 cm^{-1}, UV–vis DR spectra of the dehydrated *n*% Cu(*α*)ZSM-5 catalysts are characterized by more intense CT L–M bands in the square-planar copper oxide clusters (30,000–32000 cm^{-1}) and the weakly bound magnetic associates of $Cu^{2+}{}_{Oh}$ cations (37,500 cm^{-1}) than those of the hydrated sample. Except for NH_4^+/Cu^{2+} =0, the higher NH_4^+/Cu^{2+} ration, the lower absorbance at 30,000–32000 cm^{-1} by *n*% Cu(*α*)ZSM-5 is observed (Fig. 4C). The absorbance at 30,000–32000 and 37,500 cm^{-1} region are decreased also for the sample 1.7% Cu(6*)ZSM-5–0.33 prepared from copper–ammonia solutions with ammonium acetate addition (Fig. 4C, curve 6).

Unlike previously observed in [3], UV–vis DR bands at 22,000 and 28,000 cm^{-1} attributed to Cu-dimers [3,32,35] were not observed in the our *n*% Cu(*α*)ZSM-5 samples dehydrated under oxidizing conditions (Fig. 4C and Fig. 6, curve 1). However, weakly intensive a.b. at 22,500 and 27,900 cm^{-1} appeared in UV–vis DR spectra after dehydration of *n*% Cu(*α*)ZSM-5 in vacuum at 400 °C (Fig. 6 and curve 2). The absorbance at 22,500 cm^{-1} became stronger under subsequent high-temperature calcination of *n*% Cu(*α*)ZSM-5 in oxidizing atmosphere (Fig. 6 and curve 3). Similar changes in the UV–vis DR spectra of Cu-MFI were observed previously by Praliaud [32] and Teraoka [35]. They connected UV–vis DR band at 22,500 cm^{-1} with reoxidation of Cu^+ ions of nearby

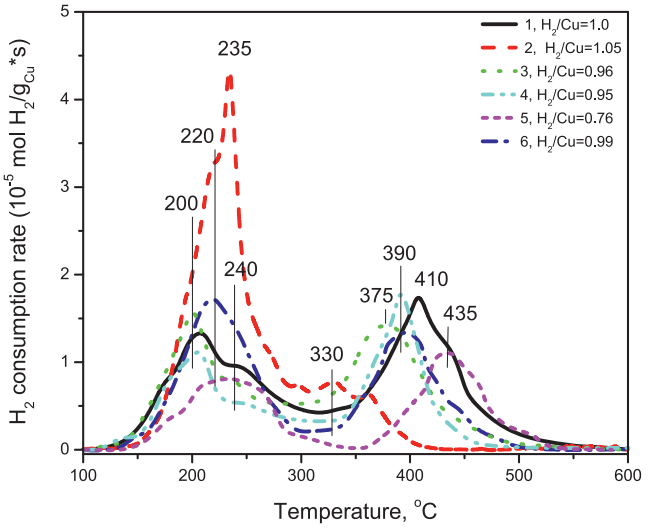

Fig. 7. H_2-TPR spectra of the ion-exchanged *n*%Cu(α)ZSM-5-*x* samples prepared at the NH_4^+/Cu^{2+} ratio equal to 0 (2 wt.% Cu, Cu/Al = 0.4, curve 1), 3 (3.5 wt.% Cu, Cu/Al = 0.68, curve 2), 6 (2.9 wt.% Cu, Cu/Al = 0.57, curve 3), 15 (2.2 wt.% Cu, Cu/Al = 0.43, curve 4) and 30 (1.85 wt.% Cu, Cu/Al = 0.36, curve 5). UV–vis DR spectra of 1.7% Cu(6*)ZSM-5–0.33 prepared from water–ammonia copper acetate solution with NH_4CH_3COO (77 g/l) are presented for comparison (curve 6).

Cu^{2+}–Cu^+ or Cu^+–Cu^+ and attributed its to CTB L → M in copper dimer bridged by extra-lattice oxygen [32,35]. Such copper pairs have to be formed due to reduction by vacuum of Cu^{2+} ions in structures with extra-lattice oxygen, for example, in dimer, chain-like and square-planar copper-oxide structures.

So, Cu-substituted ZSM-5 catalysts prepared from aqueous copper acetate solutions contain mainly isolated Cu^{2+}_{Oh} ions in zeolite cation-exchange sites. When water–ammonia solutions of copper acetate are used for synthesis of Cu-substituted ZSM-5 catalysts, in addition to isolated Cu^{2+}_{Oh} ions, the copper-oxide structures with chain-like and square-planar coordination of extra-lattice oxygen ligands are formed. These structures are located inside zeolite channels. At decreasing the ratio of ammonia to copper concentration to less than 6, the oxide clusters and CuO nanoparticles dispersed on the zeolite crystallite surface are detected in significant amount. At increasing the ratio of ammonia to copper concentration to as high as 30, the isolated Cu^{2+}_{Oh} ions become again a predominant copper state in Cu-substituted ZSM-5, but traces of copper-oxide clusters dispersed on the zeolite crystallite surface can appear due to a bonding with terminal SiOH-groups during ion-exchange mode. In our opinion, the reactions of temperature-programmed reduction by hydrogen and selective reduction of nitrous oxide by propane are most sensitive to changes in the electronic state of copper ions in Cu-substituted ZSM-5 catalysts: from isolated ions to copper ion structures with extra-lattice oxygen and CuO nanoparticles.

3.4. RedOx properties of Cu–ZSM-5 catalysts

Fig. 7 displays the curves for the temperature-programmed reduction of *n*% Cu(α)ZSM-5 catalysts synthesized by the ion-exchange of H–ZSM-5 with aqueous and water–ammonia solutions of copper acetate. The 2% Cu(0)ZSM-5–0.40 catalyst prepared from aqueous solution of copper acetate (ammonia-free solution) and containing predominantly the isolated Cu^{2+}_{Oh} ions in the cation exchange sites of the zeolite is characterized by two peak of hydrogen consumption, at 210 and 410 °C (Fig. 7, curve 1). A complete reduction of 2% Cu(0)ZSM-5–0.40 terminated at about 500–550 °C and a molar ratio H_2/Cu equal to 0.95. The H_2-TPR data show that the isolated Cu^{2+}_{Oh} ions are reduced in two steps, first to Cu^+ and then to Cu^0. Similar H_2-TPR data were reported in the literature for the ion-exchanged Cu–ZSM-5 catalysts containing isolated copper ions [9,36–38].

The 3.5% Cu(3)ZSM-5–0.68 catalyst, which was prepared at a very low ammonia content ($NH_4^+/Cu^{2+} = 3$) and had predominantly CuO nanoparticles on the external zeolite surface and minor amount of Cu^{2+}_{Oh}, is characterized by a high-intensity hydrogen absorption peak in the region of 220–240 °C and a weak-intensity peak at 330 °C (Fig. 7, curve 2). The first peak is a superposition of two H_2-consumption peaks. The sharp shape and temperature range (235–240 °C) of one of them correspond to the reduction of finely dispersed copper oxide nanoparticles. CuO is known to reduce in one stage at 220–240 °C [36,38,39] as a result of autocatalytic process [39]. The first peak includes also peak at 210–220 °C where hydrogen was consumed on reduction of isolated Cu^{2+}_{Oh} ions to Cu^+. The second step of reduction of isolated copper ions: $Cu^+ \rightarrow Cu^0$, is observed as the weak-intensity hydrogen consumption peak at 330 °C. The content of isolated Cu^{2+}_{Oh} ions observed in our work for 3.5% Cu(3)ZSM-5–0.68 catalyst was much lower as compared to 2.0% Cu(0)ZSM-5–0.40 sample; however, a complete reduction of such ions occurred at lower temperatures (420 °C versus 500–550 °C).

The *n*% Cu(α)ZSM-5 samples synthesized at moderate ammonia concentrations in copper acetate solution ($NH_4^+/Cu^{2+} = 6$–15) are also characterized by two hydrogen consumption peaks, at 200–250 °C and 375–400 °C (Fig. 7, curves 3,4), with the total hydrogen absorption corresponding to H_2/Cu close to 1. Similar to the 2.0% Cu(0)ZSM-5–0.40 catalyst, these samples contain mainly the isolated Cu^{2+}_{Oh} ions; however, their reduction starts and terminates at temperatures that are lower by 20–35 °C. When the concentration ratio NH_4^+/Cu^{2+} was decreased from 15 to 6 and then to 3, a weak tendency to the shift of the 2nd peak to the lower temperature region was observed. This indicates the improvement of reducibility of copper ions in Cu–ZSM-5. The observed shift of the reduction peaks can be attributed to stabilization of the structures of Cu^{2+} ions with extra-lattice oxygen in the zeolite channels. Probably, the beginning of their reduction to Cu^+-intermediates facilitates complete transformation of Cu^{2+} to Cu^0 due to autocatalysis. Similar phenomenon was observed for the bulk CuO [39] and assumed for Cu^{2+} ions of the over-exchanged Cu–ZSM-5 catalysts [38]. This supposition well correlates with some decrease of redox properties observed for 1.7% Cu(6*)-ZSM-5–0.33 sample (Fig. 7, curve 6). This sample was prepared from ammonia–copper solution with $NH_4^+/Cu^{2+} = 6$ and an ammonium acetate additive, introduced for suppression of hydrolysis of copper cations in solution and stabilization of the isolated Cu^{2+}_{Oh} ions in the catalyst.

For the 1.85% Cu(30)ZSM-5–0.36 catalyst synthesized at a high ammonia concentration in copper acetate solution with $NH_4^+/Cu^{2+} = 30$ and containing mainly the isolated Cu^{2+}_{Oh} ions, shift of both reduction peaks to the high-temperature region, up to 250 and 435 °C, is observed (Fig. 7, curve 5). In addition, the sample is characterized by a minimum H_2/Cu ratio equal to 0.76. Both facts indicate the most difficult reduction of isolated Cu^{2+}_{Oh} ions in the sample. The reason of reducibility deterioration is probably connected with longer distance between isolated Cu^{2+}_{Oh} ions inside zeolite channel due to low copper loading. They hardly can migrate from these positions and agglomerate, as a result, the critical size of metal copper particles is not achieved and autocatalytic reduction route does not start up. A similar reason was previously proposed to explain harder reducibility of copper ions of Cu-containing silicalite and dealuminated Y zeolite compared to Cu-substituted ZSM-5 [38]. As another reason of the poorer redox properties of 1.85% Cu(30)ZSM-5–0.36 we can consider the desilication of H–ZSM-5 during the ion exchange mode in strongly alkaline environment, namely 3 M NH_4OH in 0.1 M copper–ammonia solution. Similar desilication of H–ZSM-5 occurred in NaOH and NaOH/TPAOH solutions, though at significantly higher temperatures: 70–80°C

[40,41]. It was used for the synthesis of hierarchical zeolites with the developed mesopores [41]. Besides mesopore formation, the zeolite desilication increases the amount of SiOH-groups on external zeolite surface, changes the contribution of acidic Si(OH)Al-sites [40,41], promotes formation of intergrowth structures inside the zeolite particles [41] and accelerates loss of framework aluminium ions during thermal treatment in air [40]. Thus, in the case of the copper-substituted zeolite produced from strongly alkaline ammonia–copper solution, the decoration of CuO-like clusters by a thin silica/alumina layer during its calcination is possible due to zeolite desilication. Consequence of CuO decoration will be a decrease of the rate of hydrogen diffusion to copper ions during H_2-TPR analysis. In addition, the lower total hydrogen consumption by 1.85% Cu(30)ZSM-5–0.36 is related apparently to a formation of copper silicates, which are very difficult to reduce.

Therefore, the RedOx properties of the Cu-substituted ZSM-5 catalysts are determined by the concentration ratio NH_4^+/Cu^{2+} in copper–ammonia solution used for their preparation, because the NH_4^+/Cu^{2+} ratio affects formation of different Cu species. There are different results with *n*% Cu(α)ZSM-5 catalysts. On the one hand, moderate amount of ammonia (α = *6, 15*) was found to modify the reducibility of isolated Cu^{2+} ions of *n*% Cu(0)-ZSM-5 sample. Their reduction temperature decreased as the ammonia concentration diminished, probably due to formation of Cu-structures with extra-lattice oxygen located in zeolite channels. On the other hand, the *n*% Cu(30)ZSM-5 catalysts prepared from strong-ammonia copper acetate solution were found to be less reducible than those from ammonia-free solution and copper–ammonia solution with moderate ammonia concentration. This reducibility loss is related to the low copper loading, stabilization of isolated $Cu^{2+}{}_{Oh}$ ions with large distance between each other, decoration of copper ions by a thin silica/alumina layer or copper silicate formation. The formation of the oxide clusters and CuO nanoparticles dispersed on the zeolite crystallite surface was also proposed as a reason of change of RedOx properties of *n*% Cu(3)ZSM-5 catalysts prepared at low ammonia concentration.

3.5. Catalytic properties of Cu–ZSM-5 catalysts in SCR of NO by propane

The effect of NH_4^+/Cu^{2+} concentration ratio on properties of the Cu-substutited ZSM-5 catalysts is further illustrated by the $DeNO_x$ reactivity. The *n*% Cu(α)ZSM-5 catalysts ensure the transformation of NO to molecular nitrogen and propane to carbon dioxide and water during SCR of NO by C_3H_8. All *n*% Cu(α)ZSM-5 catalysts possess higher activity in SCR of NO by propane than H–ZSM-5 zeolite with formation of considerably smaller amounts of carbon monoxide (25–100 ppm against 800 ppm). Carbon monoxide was detected at temperatures 275–325 °C. Only trace amounts (2–10 ppm) of NO_2 were detected, principally at temperatures 250–275 °C, independently on the catalyst composition. It indicates different mechanisms of NO reduction by propane over pure and copper-modified H–ZSM-5 zeolite.

The catalytic behaviours: NO conversion, propane conversion, CO_2 formation, and C_3H_8 consumption in NO reduction for a series of 2% Cu(α)ZSM-5 catalysts prepared at a variation of the NH_4^+/Cu^{2+} ratio in ion-exchange solution of copper acetate and containing about 2 wt.% of copper are given in Fig. 8. Curves of NO conversion, C_3H_8 conversion, and CO_2 formation versus temperature have a S-shaped form. Among catalysts 2% Cu(α)ZSM-5, the catalyst 2.3% Cu(6)ZSM-5–0.45 possessed the lowest temperatures of achievement of 50% and 99% conversion of nitrogen oxide, they amounted to 265 and 300 °C, respectively (Fig. 8A, curve 3). The temperature of 50% conversion of NO over other 2% Cu(α)ZSM-5 raised with NH_4^+/Cu^{2+} ratio in the following sequence: α6 (265 °C) < α15 (275 °C) < α30 (280 °C) < α3 ~ α0 (290 °C) (Fig. 8A). Thus, it is possible to make the assumption that copper ions with extra-framework oxygen (as in 2.3% Cu(6)ZSM-5–0.45) have the maximum activity in NO reduction, while the $DeNO_x$ activity of the isolated copper ions (by analogy with 2.0% Cu(0)ZSM-5–0.40) and CuO nanoparticles on an external zeolite surface (as in 2.0% Cu(3)ZSM-5–0.40) is somewhat lower.

At temperature above 375 °C, however, NO conversion over catalyst 2.3% Cu(6)ZSM-5–0.45 significantly decreased and amounted to about 90% at 550 °C. Similar lowering of NO conversion was observed for all 2% Cu(α)ZSM-5 catalysts which had been prepared from water–ammonia solutions of copper acetate with low and moderate concentration of ammonia (Fig. 8A, curves 2 and 4); while it was practically absent (from 99% to 97%, Fig. 8A, curve 5) in $DeNO_x$ behavior of the catalyst 2% Cu(30)ZSM-5–0.4 prepared from solution with high ammonia concentration. The falling of the NO conversion in high-temperatures region is associated with the propane transformation in the competing reactions of its deep oxidation, resulting C_3H_8/NO ratio considerably diminishes and propane concentration in the feed does not suffice for the NO reduction. It is reliably established that low values of the C_3H_8/NO ratio has detrimental effect on $DeNO_x$ activity of Cu-substituted zeolite [42].

The activity of 2% Cu(α)ZSM-5 catalysts in propane transformation during SCR of NO is also affected by NH_4^+/Cu^{2+} concentration ratio. Propane reacts more difficultly over 2% Cu(0)ZSM-5–0.4 catalyst compared with other Cu-substituted catalysts prepared from water–ammonia solution of copper acetate. So, the catalyst 2% Cu(3)ZSM-5–0.4 provides 99% propane conversion at 335–340 °C, while the 2% Cu(0)ZSM-5–0.4 catalyst does it only at about 360 °C (Fig. 8B, curves 1 and 2). At lower propane conversions, a sequence of changes in the activity of 2% Cu(α)ZSM-5 as a function of NH_4^+/Cu^{2+} ratio is similar to that observed for the NO conversion. The temperature of 50% propane conversion over catalysts increased with NH_4^+/Cu^{2+} ratio as: α6 (285 °C) < α15 (295 °C) < α30 (305 °C) < α3 (310 °C) < α0 (315 °C) (Fig. 8B). The CO_2 emissions over 2% Cu(α)ZSM-5 catalysts with different NH_4^+/Cu^{2+} ratio is characterized by similar trends (Fig. 8D). By analogy with the NO removal, the reactivity inequality of propane conversion over 2% Cu(α)ZSM-5 catalysts can be explained by the different structure of the copper active sites that have different oxidation potential. For the sample 2% Cu(3)ZSM-5–0.4, they are the Cu-oxide clusters and CuO nanoparticles dispersed on the zeolite crystallite surface; while in the sample 2% Cu(0)ZSM-5–0.4 they are identified as isolated $Cu^{2+}{}_{Oh}$ ions. The former is well known [32,43,44] for their higher activity in deep hydrocarbons oxidation compared to the isolated copper ions.

It is seen in Fig. 8C the selectivity of propane consumption in NO reduction over 2% Cu(α)ZSM-5 catalysts grows with a temperature increase, but reaching a maximum value declines and does not exceed 10% for all catalysts at temperatures above 360 °C. Low propane selectivity indicates that the rate of the deep propane oxidation greatly exceeds the rate of propane consumption in NO SCR at high temperatures. The propane selectivity top and its temperature (Fig. 8C) change at variation of the NH_4^+/Cu^{2+} ratio of the ion-exchange solution. For example, all ex-copper–ammonia 2% Cu(α)ZSM-5 catalysts have higher propane consumption selectivity compared with the catalyst prepared from ammonia-free solution. In the temperature range 240–290° C, its value stood at 40–60% for 2% Cu(3–30)ZSM-5 compared to 25–30% found for 2% Cu(0)ZSM-5–0.4 catalyst.

Thus, the change in the copper electronic state: from the isolated copper ions to the structures of copper ions with extra-framework oxygen located in zeolite channels and the oxide clusters and the CuO nanoparticles dispersed on the zeolite crystallite surface, observed when we varied the NH_4^+/Cu^{2+} ratio of ion-exchange solution, strongly modifies both $DeNO_x$ and propane conversion

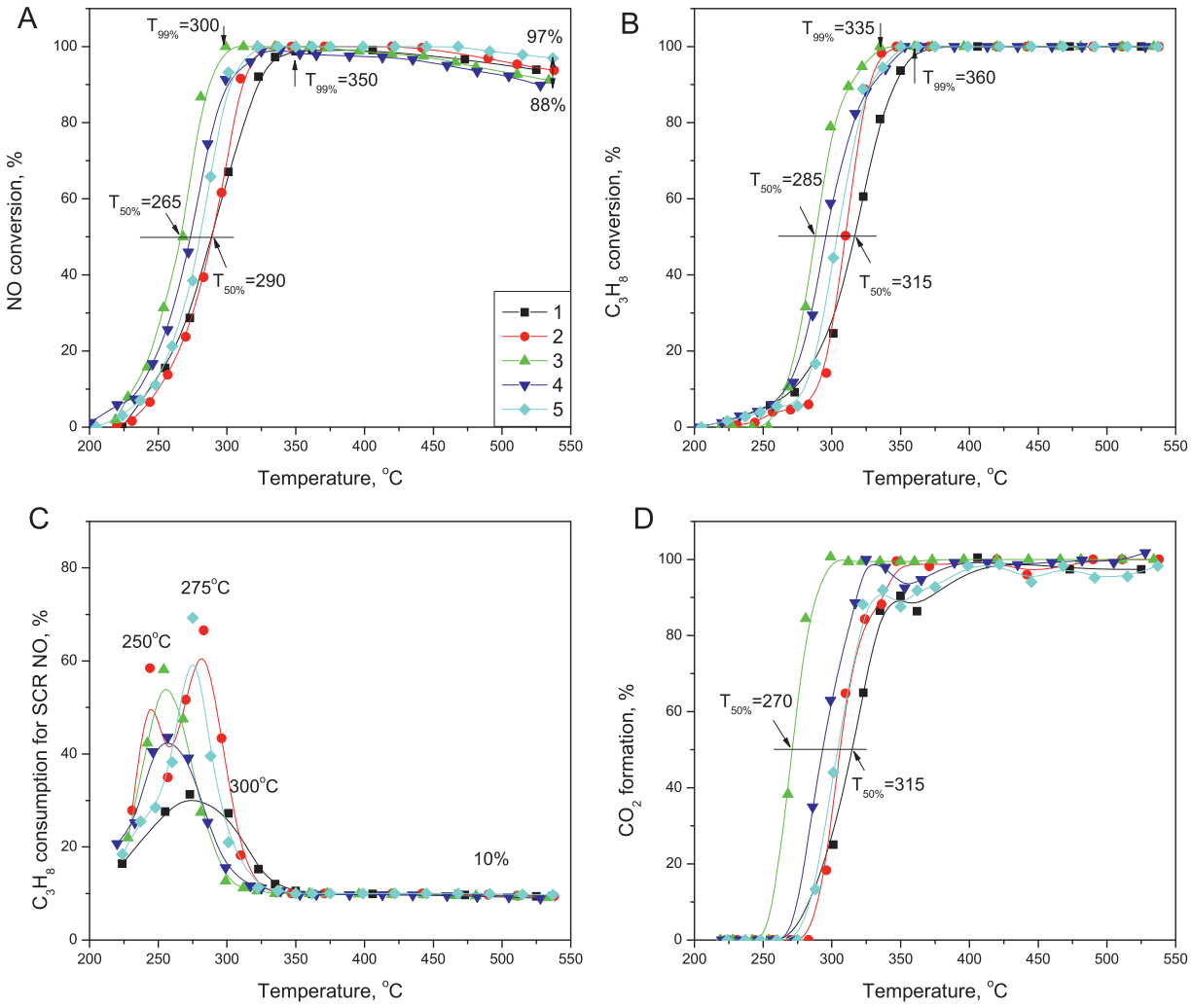

Fig. 8. NO conversion (A), C_3H_8 conversion (B), C_3H_8 consumption for SCR of NO (C) and CO_2 formation (D) during SCR NO-C_3H_8 reaction over the ion-exchanged 2% Cu(α)ZSM-5–0.4 samples prepared at NH_4^+/Cu^{2+} ration equal to 0 (curve 1), 3 (curve 2), 6 (curve 3), 15 (curve 4) and 30 (curve 5).

activity of 2% Cu(α)ZSM-5 catalysts. Since it is difficult to synthesize Cu-substituted ZSM-5 catalysts with a single copper electronic state via the ion exchange mode, we have attempted to make the correlation between the rate constant of nitric oxide and propane conversion over *n*% Cu(α)ZSM-5 catalysts and total copper loading in order to identify the contribution of specific copper states in the catalytic activity. These correlations have been made for temperature 275 °C (Fig. 9), at which most of the catalysts provided 20–50% conversion of nitric oxide and 5–20% conversion of C_3H_8, and reaction products: CO_2 and H_2O, quickly desorbed from active copper sites.

To start with, it is worth noting that H–ZSM-5 zeolite as well as the zeolite pretreated in ammonia solution (whose concentration was the same as in the copper–ammonia solution with $NH_4^+/Cu^{2+}=30$) have non-zero activity in the NO reduction and propane oxidation. The rate constant of NO reduction over these zeolites reached 6.7 $s^{-1}g_{cat}^{-1}$. Their rate constants of C_3H_8 transformation were 0.66 and 3.2 $s^{-1}g_{cat}^{-1}$, respectively. Therefore, the rate constants of NO and propane transformation as function of copper loading, $k_{NO}=f(Cu)$ and $k_{C3H8}=f(Cu)$, do not pass through the origin (Fig. 9A and C). The $DeNO_x$ activity of zeolites without copper is due to iron ions, which are present in the amount of 0.09 wt.%. We noticed that the pretreatment of H–ZSM-5 in the concentrated ammonia leads to desilicious surface and the formation of mesopores, but it does not affect on its $DeNO_x$ activity.

It is seen in Fig. 9A, the k_{NO} value in the presence of *n*% Cu(0)ZSM-5 and *n*% Cu(30)ZSM-5 catalysts is not changed in comparison with the copper-free zeolites, until the copper loading is lower than 0.75–0.80 wt.%. After that, k_{NO} has a proportional increase with increasing of the copper content in the catalyst. For the *n*% Cu(α)ZSM-5 catalysts prepared at $NH_4^+/Cu^{2+}=0$ and 30, the proportionality factor (a, $*10^{-2}$ $s^{-1}g_{Cu}^{-1}$) of their $k_{NO}=f(Cu)$ correlations have the same values equal to 10.2. It should be noted that $DeNO_x$ activity of *n*% Cu(0)ZSM-5 catalysts prepared by the ion exchange of NH_4-ZSM-5 and Na-ZSM-5 zeolites with copper acetate solution are approximated also well by this correlation (Fig. 9A, curves 2 and 3).

Similar trends were observed for k_{C3H8} in the presence of the catalysts' series prepared at $NH_4^+/Cu^{2+}=0$ and 30 (Fig. 9C). The copper loading dependence of k_{C3H8} for *n*% Cu(0)ZSM-5 and *n*% Cu(30)ZSM-5 catalysts have the same slope (a, $*10^{-2}$ $s^{-1}g_{Cu}^{-1}$) equal to 1.9 and 1.8, respectively.

According to ESR, UV–vis DR and TPR-H_2 results discussed above, the *n*% Cu(0)ZSM-5 and *n*% Cu(*30*)ZSM-5 samples contain predominantly isolated Cu^{2+} ions. Their number increases as the copper content in the catalyst reaches Cu/Al = 0.5. Thus, data correlation shows that $DeNO_x$ reactivity of the series of *n*% Cu(0)ZSM-5 and *n*% Cu(30)ZSM-5 catalysts raises with increasing concentration of isolated Cu^{2+} ions in the sample. Therefore, the maximum achievable activity is limited to the amount of the isolated Cu^{2+}

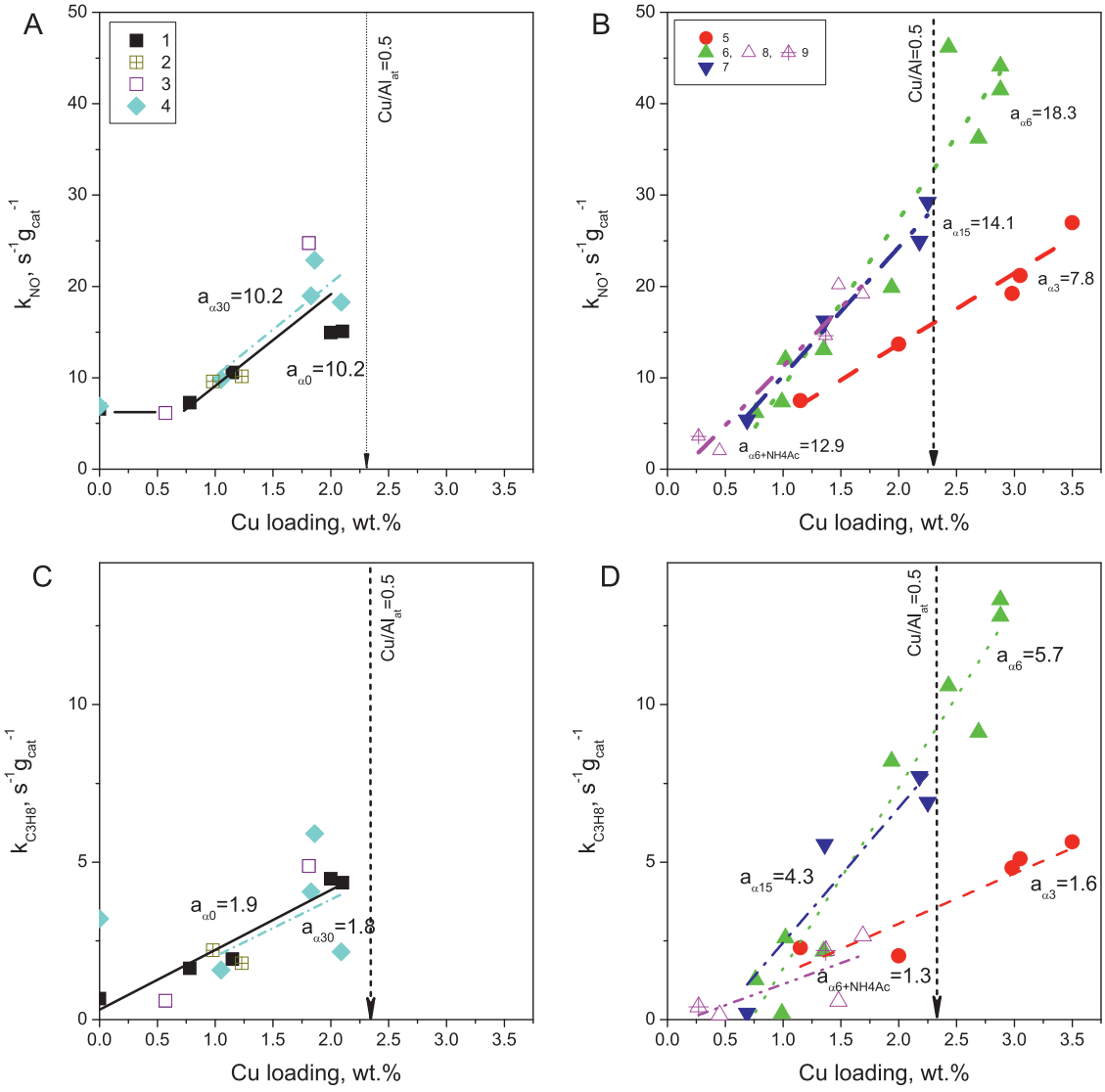

Fig. 9. Rate constant of NO (A and B) and propane (C and D) conversion over *n*% Cu(*α*)ZSM-5 catalysts at 275 °C. The *n*% Cu(*α*)ZSM-5 samples have been prepared by the ion-exchange of H–ZSM-5 (curves 1, 4–9), NH_4-ZSM-5 (curve 2) or Na-ZSM-5 (curve 3) with water-ammonia solution of copper acetate at NH_4^+/Cu^{2+} ratio (*α*) equal to 0 (curves 1, 2, 3), 3 (curve 5), 6 (curve 6, 8, 9), 15 (curve 7) and 30 (curve 4), including those containing additive of 1 M (curve 8) and 3 M (curve 9) of ammonium acetate. a_α(*10^{-2} $s^{-1}g_{Cu}^{-1}$*) is slope of correlation between k_{NO} or k_{C3H8} and copper content for each NH_4^+/Cu^{2+} ratio.

ions that can be introduced by the stoichiometric ion exchange, i.e., Cu/Al = 0.5.

It is seen in Fig. 9B and D, the different result was obtained with other catalysts series prepared at the NH_4^+/Cu^{2+} ratio in the range from 3 to 15. Their dependences of k_{NO} and k_{C3H8} on copper content have two features. First, the intercepts on k_{NO} and k_{C3H8} axes are zero. Second, the slopes differ from the slope observed for the catalysts' series with NH_4^+/Cu^{2+} equal to 0 and 30. So, for the series of *n*% Cu(3)ZSM-5 catalysts, the slope of k_{NO} and k_{C3H8} were less than these values. They amounted to 7.8 and 1.6, respectively (Fig. 9B and D, curve 5). By contrast, the catalysts series *n*% Cu(6)ZSM-5 had slopes of k_{NO} and k_{C3H8} in 2–3 times more (Fig. 9B and D, curve 6). The change of the NH_4^+/Cu^{2+} ratio from 6 to 15 led to a decrease of the k_{NO} and k_{C3H8} slopes, up to 14.1 and 4.3, respectively (Fig. 9B and D, curve 7).

The rate constants of NO and propane conversion over *n*% Cu(6*)ZSM-5 catalysts, which were prepared from the water–ammonia solution of copper acetate with 1 M and 3 M ammonium acetate adding, are well approximated by a linear dependence on copper loading and characterized by similar proportionality factor (Fig. 9B and D, curves 8 and 9). Their k_{NO} slope was smaller compared with that for *n*% Cu(6)ZSM-5 catalysts prepared without such additives (12.9 against 18.3). Conversely, its value was close to that of the *n*% Cu(0)ZSM-5 and *n*% Cu(*30*)ZSM-5 catalysts (Fig. 9A). In addition, their k_{C3H8} slope had the smallest value among the studied catalysts (Fig. 9D, curve 8,9). For example, it is nearly 5 times lower in comparison with that typical for *n*% Cu(6)ZSM-5 catalyst series.

Therefore, variation of the NH_4^+/Cu^{2+} ratio at *n*% Cu(α)ZSM-5 catalysts synthesis modifies the $DeNO_x$ reactivity as well as copper electronic state. From these correlations we can deduce that the copper structures with extra-lattice oxygen inside zeolite channels show the maximum reactivity both in NO removal and propane oxidation. Their high $DeNO_x$ reactivity is caused, apparently, by the high covalence of Cu–O bond and by the stabilization of the mixed-valence state of Cu(II)–Cu(I) at a slightly reducing environment. The latter are good electron donors that facilitate the formation of σ-bond with NO and its transformation [46].

From ESR, UV–vis DR and TPR-H_2 results, we assume that the maximum concentration of Cu-structures with extra-lattice oxy-

gen is formed in the over-exchanged *n*% Cu(α)ZSM-5 catalysts prepared at moderate ammonia concentrations. That is why the over-exchanged *n*% Cu(6)ZSM-5 catalysts possess the higher catalytic activity among studied catalysts (Fig. 9B and Fig. 9D, curve 6 at Cu/*Al* > 0.5). The tendency to diminution of $DeNO_x$ activity, that we observed at increasing the NH_4^+/Cu^{2+} ratio of copper–ammonia solution from 6 to 15 (Fig. 9B, curves 7–9), can be explained by the decrease in the number of Cu-structures with extra-lattice oxygen and the increase of concentration of isolated Cu^{2+} ions.

For understanding which of the specific copper states gives more to the catalytic activity, the $DeNO_x$ activity of a series of catalysts *n*% Cu(6*)ZSM-5 prepared by adding ammonium acetate to the ammonia–copper solution with $NH_4^+/Cu^{2+} = 6$, were investigated. According to AES-ICP and UV–vis DR data, ammonium acetate is believed to lessen copper loading and promote stabilization of the isolated $Cu^{2+}{}_{Oh}$ ions in the ion-exchanged *n*% Cu(6*)ZSM-5 catalysts due to suppression of hexaaquacopper(II) cations hydrolysis in copper–ammonia solutions. A comparison of catalytic activity of the under-exchanged catalysts *n*% Cu(6)ZSM-5 and *n*% Cu(6*)ZSM-5 (Fig. 9B, curves 6, 8 and 9 at Cu/Al < 0.5) shows that the $DeNO_x$ activity of the isolated $Cu^{2+}{}_{Oh}$ ions is a little less or even comparable with the activity of the Cu-structures with extra-lattice oxygen located in zeolite channels, while they have significantly lower activity in propane oxidation. Note that the isolated $Cu^{2+}{}_{Oh}$ ions dominate in the under-exchanged Cu–ZSM-5 (with $Cu/Al_{at} < 0.2$ [5]), while the Cu-structures with extra-lattice oxygen prevail in the over-exchanged Cu–ZSM-5 catalysts (with $Cu/Al_{at} > 0.5$ [5]).

The minimum activity in both the NO reduction and the propane oxidation is typical for the Cu oxide clusters and CuO nanoparticles dispersed on the zeolite crystallite surface. They were observed by electronic spectroscopy in the *n*% Cu(3)ZSM-5 catalysts, which had been prepared from weak-ammonia solutions of copper acetate and had the low $DeNO_x$ catalytic activity (Fig. 9B and D, curve 5). The low $DeNO_x$ reactivity of the Cu oxide clusters and CuO nanoparticles is connected with their ability to activate oxygen much more readily than NO, and bring about a deep propane oxidation. In addition, the CuO-like clusters and CuO nanoparticles are more reducible in TPR-H_2 experiment than Cu-structures with extra-lattice oxygen. Therefore, they possess higher labile oxygen, which can be used on propane oxidation. This is probably the other reason of their low $DeNO_x$ activity. This hypothesis agrees with well-known fact that highly dispersed copper species on inert oxide matrix can reduce NO to N_2, while large CuO-like clusters do not [32,45].

4. Conclusions

It was demonstrated that the NH_4^+/Cu^{2+} concentration ratio in copper–ammonia solution determined reducibility of Cu-species as well as $DeNO_x$ activity of Cu-substituted ZSM-5 through different Cu states and copper loading. During the ion exchange, an increase in the copper acetate concentration in both the aqueous and ammonia solutions naturally increased Cu content in the zeolite; however, the maximum amount of copper adsorbed from ammonia-free, moderate-concentrated and strong-ammonia solutions is limited by the number of cation exchange sites, the dynamic adsorption equilibrium, and the presence of competing cations capable of exchanging with the cation exchange sites of the zeolite (for example, NH_4^+, $[Cu_2(OH)_2]^{2+}{}_{aq}$). The copper(II) complexes introduced inside zeolite channels during this ion-exchange mode are stabilized as the isolated Cu^{2+} ions and Cu-structures with extra-lattice oxygen. When weak-ammonia solution of copper acetate ($NH_4^+/Cu^{2+} < 6$) is used for ion-exchange, the copper loading in Cu–ZSM-5 increases, but the copper oxide clusters and CuO nanoparticles dispersed on the zeolite crystallite surface are mainly formed due to polycondensation or the so-called "core-plus-links" reaction.

The comparison of the catalytic activity of Cu–ZSM-5 in SCR of NO by propane with different electronic states of copper indicates that the dynamics of their $DeNO_x$ activity correlates with the growth of the number of isolated copper ions and Cu-structures with extra-lattice oxygen. The latter structures are more readily reducible than the isolated copper ions and less reducible compared with the copper oxide clusters and CuO nanoparticles dispersed on the zeolite crystallite surface.

Acknowledgement

ESR spectra were recorded using spectrometer located in Kemerovo multi-user center of scientific equipment. The authors thank Ivanov A. for conducting ESR investigation (Kemerovo).

References

[1] M. Iwamoto, H. Yahiro, Y. Mine, S. Kagawa, Chem. Lett. 2 (1989) 213–216.
[2] W. Held, A. Konig, T. Richter, L. Puppe, SAE Tech. Paper Ser. 900496 (1990) 13–18.
[3] M.H. Groothaert, J.A. van Bokhoven, A.A. Battiston, B.M. Weckhuysen, R.A. Schoonheydt, J. Am. Chem. Soc. 125 (2003) 7629–7640.
[4] S.A. Yashnik, Z.R. Ismagilov, V.F. Anufrienko, Catal. Today 110 (2005) 310–322.
[5] A. Kubacka, Z. Wang, B. Sulikowski, J. Catal. 250 (1) (2007) 184–189.
[6] O.P. Taran, S.A. Yashnik, A.B. Ayusheev, A.S. Piskun, R.V. Prihod'ko, Z.R. Ismagilov, V.V. Goncharuk, V.N. Parmon, Cu-containing MFI zeolites as catalysts for wet peroxide oxidation of formic acid as model organic contaminant, Appl. Catal. B: Environ. 140–141 (2013) 506–515.
[7] S.M. Ciocılteu, M. Salou, Y. Kiyozumi, F. Sh Niwa, Mizukami, M. Haneda, J. Mater. Chem. 13 (2003) 602–607.
[8] O.P. Krivoruchko, T.V. Larina, R.A. Shutilov, V. Yu Gavrilov, S.A. Yashnik, V.A. Sazonov, I. Molina, Z.R. Ismagilov, Appl. Catal. B: Environ. 103 (2011) 1–12.
[9] S.A. Yashnik, A.V. Salnikov, N.T. Vasenin, V.F. Anufrienko, Z.R. Ismagilov, Catal. Today 197 (2012) 214–227.
[10] M. Iwamoto, H. Yahiro, Y. Torikai, T. Yoshioka, N. Mizuno, Chem. Lett. (1990) 1967–1970.
[11] J. Valyon, W.K. Hall, Catal. Lett. 19 (1993) 109–119.
[12] Y. Zhang, K.M. Leo, A.F. Sarofim, Z. Hu, M. Flytzani-Stephanopoulos, Catal. Lett. 31 (1995) 75–89.
[13] L.T. Tsikoza, E.V. Matus, Z.R. Ismagilov, V.A. Sazonov, V.V. Kuznetsov, Kinet. Catal. 46 (4) (2005) 613–617.
[14] A.V. Kucherov, J.L. Gerlock, H.-W. Jen, M. Shelef, Zeolites 15 (1995) 9–14.
[15] J. Dedecek, B. Wichterlova, J. Phys. Chem. 10 (1997) 233–10240, B. 101.
[16] S.C. Larsen, A. Aylor, A.T. Bell, J.A. Reimer, J. Phys. Chem. 98 (44) (1994) 11533–11540.
[17] M. Iwamoto, H. Yahiro, K. Tanda, N. Mizuno, Y. Mine, S. Kagawa, J. Phys. Chem. 95 (1991) 3727–3730.
[18] Y. Kuroda, A. Kotani, H. Maeda, H. Moriwaki, T. Morimato, J. Chem. Soc. Faraday Trans. 88 (11) (1992) 1583–1590.
[19] E.S. Shapiro, W. Gruner, R.W. Joyner, G.N. Baeva, Catal. Lett. 24 (1994) 59–169.
[20] M. Iwamoto, H. Yahiro, N. Mizumo, W.-X. Zhang, Y. Mine, H. Furukawa, S. Kagawa, J. Phys. Chem. 96 (1992) 9360–9366.
[21] C. Torre-Abreu, M.F. Ribeiro, C. Henriques, F.R. Ribeiro, Appl. Catal. B: Environ. 11 (1997) 383–401.
[22] M. Iwamoto, H. Yahiro, S. Shundo, Y. Yu-u, N. Mizuno, Appl. Catal. A: Gen. 69 (1991) L15–L19.
[23] D.D. Perrin, J. Chem. Soc. (1960) 3189–3196.
[24] C.F. Baes Jr., R.E. Mesmer, The Hydrolysis of cations. – New York: Wiley, Interscience (1976) 267–274.
[25] J. Vazquez-Arenas, I. Lazaro, R. Cruz, Electrochim. Acta 52 (2007) 6106–6117.
[26] I. Giannopoulou, D. Panias, I. Paspaliaris, Hydrometallurgy 99 (2009) 58–66.
[27] A.B.P. Lever, Inorganic Electron Spectroscopy, Vol. 2, Elsevier, 1984, 2015.
[28] N.N. Tikhomirova, K.I. Zamaraev, V.M. Berdnikov, J. Struct. Chem. (Engl. Transl.) 4 (1963) 407–411.
[29] Y. Li, W.K. Hall, J. Catal. 129 (1991) 202–215.
[30] G. Martini, L. Burlamacchi, J. Phys. Chem. 83 (1979) 2505–2511.
[31] G. Moretti, C. Dossi, A. Fusi, S. Recchia, R. Psaro, Appl. Catal. B: Environ. 20 (1999) 67–73.
[32] H. Praliaud, S. Mikhailenko, Z. Chajar, M. Primet, Appl. Catal. B: Environ. 16 (1998) 359–374.
[33] I. Dedecek, O. Bortnovsky, A. Vondrova, B. Wichterlova, J. Catal. 200 (2001) 160–170.
[34] S.A. Bates, A.A. Verma, C. Paolucci, A.A. Parekh, T. Anggara, A. Yezerets, W.F. Schneider, J.T. Miller, W.N. Delgass, F.H. Ribeiro, J. Catal. 312 (2014) 87–97.
[35] Y. Teraoka, C. Tai, H. Ogawa1, H. Furukawa, S. Kagawa, Appl. Catal. A: Gen. 200 (2000) 167–176.

[36] J. Sarkany, J.L. d'Itri, W.M.H. Sachtler, Catal. Lett. 16 (1992) 241–249.
[37] R. Bulanek, B. Wichterlova, Z. Sobalık, J. Tichy. Appl. Catal. B: Environ. 31 (2001) 13–25.
[38] O.P. Tkachenko, K.V. Klementiev, M.W.E. van den Berg, N. Koc, M. Bandyopadhyay, A. Birkner, C. Woll, H. Gies, W. Grunert, J. Phys. Chem. B 109 (2005) 20979–20988.
[39] J.A. Rodriguez, J.Y. Kim, J.C. Hanson, M. Perez, A.I. Frenkel, Catal. Lett. 85 (2003) 247–254.
[40] K. Barbera, F. Bonino, S. Bordiga, T.V.W. Janssens, P. Beato, J. Catal. 280 (2011) 196–205.
[41] K. Sadowska, A. Wach, Z. Olejniczak, P. Kusтrowski, J. Datka, Micropor. Mesopor. Mater. 167 (2013) 82–88.
[42] R. Gopalakrishnan, P.R. Stafford, J.E. Davidson, Appl. Catal. B: Environ. 2 (1993) 165–182.
[43] A.K. Neyestanaki, N. Kumar, L.-E. Lindfors, Fuel 74 (5) (1995) 690–696.
[44] O. M'Ramadj, B. Zhang, D. Li, X. Wang, G. Lu, J. Nat. Gas Chem. 16 (2007) 258–265.
[45] H.H. Kung, M.C. Kung, Catal. Today 30 (1996) 5–14.
[46] I.I. Zakharov, Z.R. Ismagilov, S.Ph. Ruzankin, V.F. Anufrienko, S.A. Yashnik, O.I. Zakharova, J. Phys. Chem. C 111 (2007) 3080–3089.